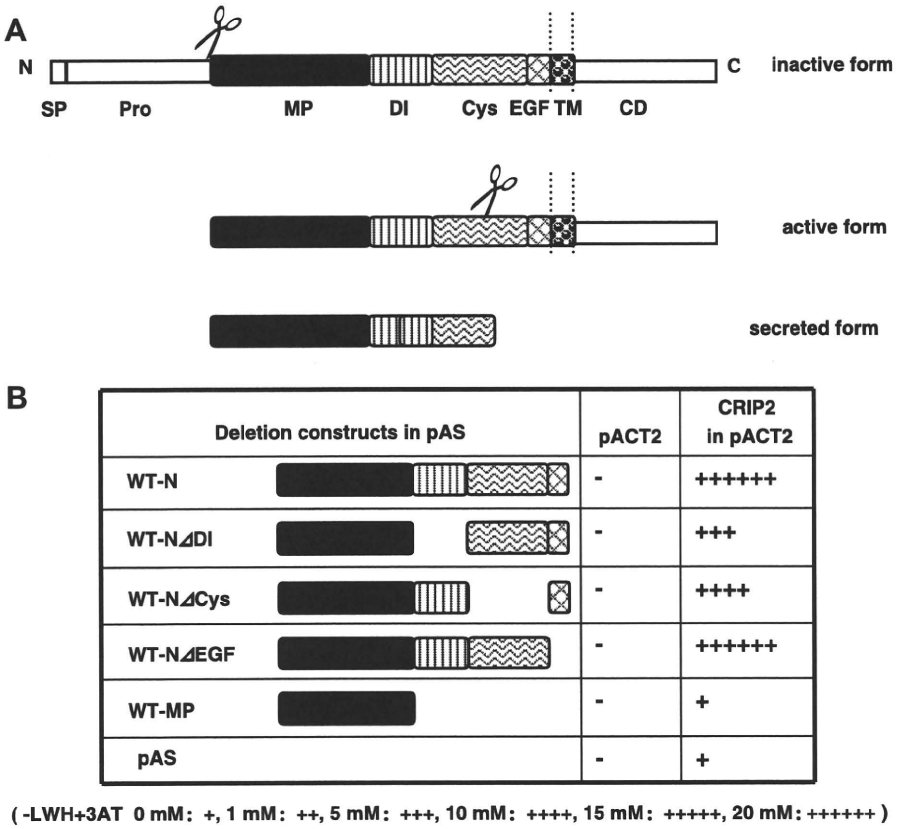

Fig. 1. Yeast two-hybrid screening with the extracellular domain of ADAM19. (A) Schematic of the domain structure and processing of ADAM19. ADAM19 is inactive in the presence of the pro-domain (Pro). Proteolytic removal of the pro-domain by furin activates the metalloprotease domain (MP) and produces the active form of ADAM19, followed by autolysis in the cysteine-rich domain (Cys) to produce a secreted form. (B) The binding of CRIP2 to various domain-deletion mutants of ADAM19 was compared by 3AT-assay. The number of pluses (+) represents the degree of binding based on the highest concentration of 3AT (on plates lacking His, Leu, and Trp) that allowed cellular growth: 1, 2, 3, 4, 5, and 6 pluses indicate 0, 1, 5, 10, 15, and 20 mM 3AT, respectively. A minus (−) indicates no cell growth on the plates.

CRIP2 increased in parallel with the autolytic processing of ADAM19 stimulated by lipopolysaccharide (LPS). These findings suggest that ADAM19 autolysis is activated by LPS and that ADAM19 promotes non-classical secretion of CRIP2.

2. Materials and methods

2.1. Vectors and constructs

Human ADAM19 transcript variant 2, excluding the stop codon, was inserted into pcDNA3.1/V5-HisA (Invitrogen), which had been digested by EcoRV and XbaI, after the addition of GCCACC as a Kozak sequence. The V5 epitope tag was fused at the C-terminus.

ADAM19EA-N, the N-terminus of ADAM19 containing catalytically inactive mutant E346A, from the MP domain to the EGF domain, was inserted into the pAS2-1C vector as bait. The following domains were inserted into the pAS2-1C vector: WT-N (wild-type ADAM19 N-terminus from the MP domain to the EGF domain), WT-NΔDI (WT-N with the DI domain deleted), WT-NΔCys (WT-N with the Cys domain deleted), WT-NΔEGF (WT-N with the EGF domain deleted), and WT-MP (the MP domain).

Human CRIP2 was amplified from a human fetal brain cDNA library (TaKaRa) and inserted into pBluescript SK+(Stratagene). The coding region was reconstructed with pCMV-HA (TaKaRa) to fuse the HA tag at the N-terminus, and with pcDNA3.1–Myc to fuse the Myc tag at the N-terminus. The pcDNA3.1–Myc vector was made by inserting six tandem repeats of the Myc tag into pcDNA3.1(+) (Invitrogen), between the EcoRV and XhoI sites.

2.2. Antibodies and reagents

The following antibodies were purchased: anti-CRIP2 (sc-30272) and HRP-conjugated donkey anti-goat IgG (sc-2020) (Santa Cruz Biotechnology, Inc.); anti-V5 antibody (Invitrogen); anti-HA antibody (Roche); and anti-Myc antibody, HRP-conjugated anti-mouse IgG, and anti-rabbit IgG (Cell Signaling Technology). The 76-amino acid C-terminal fragment of ADAM19 was purified using glutathione Sepharose (GE Healthcare Bio-Science Corp.), for use as an antigen in rabbits. Approximately 1 mg of the antigen in complete Freund's adjuvant (Wako) was injected into a rabbit, and after 1 month, the rabbit was boosted with an additional 1 mg. Blood was collected from the rabbit, the serum was clarified with ammonium sulfate, and the antibody was purified with antigen-bound Affi-Gel 10 (Bio-Rad).

Lipopolysaccharides from *Escherichia coli* 055:B5 were purchased from Sigma–Aldrich.

2.3. Cell culture

COS-7, human neuroglioma H4, and human glioblastoma A172 cells were cultured in DMEM (Sigma–Aldrich) supplemented with 10% fetal bovine serum (Gibco). The cells were maintained at 37 °C in an atmosphere of 5% CO_2 in a tissue culture incubator. H4 cells stably expressing human ADAM19–V5 or pcDNA3.1/V5-HisA vector were cloned and cultured in medium containing G418 at 0.1 mg/mL.

2.4. RNA interference

When 50% confluent, A172 cells were transfected with hADAM19 stealth RNA or control random RNA (100 pmol/6-cm dish) using Lipofectamine 2000 (Invitrogen) and OPTI-MEM I (Gibco). The following target sequences were used in this study: sense, GGGCCAACACCUUAUUUACAGAUCU; and anti-sense, AGAUCUG UAAAUAAGGUGUUGGCCC. Stealth RNAi Negative Control Low GC Duplex (Invitrogen) was used as a negative control.

2.5. Cell lysis and protein concentration

Cells were collected and lysed on ice in TNE lysis buffer (25 mM Tris–HCl, pH 7.5, 150 mM NaCl, 5 mM EDTA, 1% NP-40) containing a protease inhibitor mixture. Cell disruption was completed by three freeze–thaw cycles. Following centrifugation at 16,000g for 10 min at 4 °C, the protein concentration in the supernatant was quantified using a DC protein assay kit (Bio-Rad). The protein was concentrated by precipitation with 10% trichloroacetic acid.

2.6. Western blot analysis

Protein samples were separated by 10% SDS–PAGE and transferred to PVDF membranes (Immobilon-P; Millipore). The membranes were soaked in 5% nonfat dried milk in PBS with 0.05% Tween for 1 h and then incubated with primary antibodies in PBS containing 0.05% Tween, 0.1% BSA, and 1 mM NaN_3 overnight at 4 °C. After washing, the membranes were incubated with HRP-conjugated secondary antibody for 1 h. The antigen–antibody complex was detected by enhanced chemiluminescence using a Luminescent image analyzer LAS-3000 (Fujifilm). The magnitude of the signal was digitized using Multi Gauge Ver. 2.3 software (Fujifilm).

2.7. Immunoprecipitation

COS-7 cells overexpressing human ADAM19–V5 or Myc–human CRIP2 were solubilized in HEPES lysis buffer (20 mM HEPES, pH 7.5, 150 mM NaCl, 0.1% CHAPS) containing 1 mM PMSF and a protease inhibitor mixture (Sigma–Aldrich). The homogenate was passed through a 27-gauge needle (10 times) and rotated for 15 min, followed by centrifugation at 100,000g for 30 min at 4 °C. Supernatant samples containing equal amounts of protein were transferred to new tubes and pre-cleared by incubation with Protein A Sepharose beads (GE Healthcare Bio-Science Corp.) for 1 h at 4 °C. Proteins were immunoprecipitated overnight using anti-V5 antibody (Invitrogen) and anti-mouse IgG. The antibody-bound complexes were isolated by incubation with Protein A Sepharose beads for 2 h and then washed three times in HEPES lysis buffer. The protein complexes were eluted in 2× SDS sample buffer and analyzed by Western blotting with a polyclonal anti-Myc antibody.

2.8. Immunocytochemistry

A172 cells overexpressing HA–CRIP2 were fixed with 4% paraformaldehyde in PBS, blocked with 5% BSA, and immunostained with anti-HA antibody and an Alexa 488-conjugated secondary antibody without membrane permeabilization. The cells were observed under a fluorescence microscope (Model X171; Olympus).

2.9. Yeast two-hybrid screening

Yeast two-hybrid screening was performed with a MATCHMAKER GAL4 Two-Hybrid System (Clontech). AH109 yeast cells were transformed with ADAM19EA-N in pAS using the LiAc method, followed by transformation with a human fetal brain cDNA library in pACT2 vector. The transformation efficiency was about 1,872,000 cfu/μg. We obtained 1179 positive colonies by selection on −LWHA plates and −LWH + 5 mM 3-aminotriazole (3AT) plates, and by β-galactosidase assay. The binding intensity was evaluated by 3AT assay.

3. Results

3.1. Yeast two-hybrid screening with extracellular domains of ADAM19

To identify a new physiological function of ADAM19, we screened for proteins that associate with ADAM19 using a yeast two-hybrid system. We constructed a bait, EA-N, that consisted of extracellular domains from the metalloprotease domain to the EGF-like domain, including a catalytically inactive mutant of the metalloprotease domain (E346A), and found several candidate binding molecules, in addition to the known ADAM inhibitor TIMP-3. The cDNAs were extracted from the yeast cells and purified. Yeast cells were re-transformed with bait, and the binding intensity was examined by 3-AT assay. To confirm the binding, the bait and prey were switched. As a result, cysteine-rich protein 2 (CRIP2) [GenBank: NM_001312] was identified as a candidate protein.

We analyzed determined the domains of ADAM19 that were recognized by CRIP2. The binding of CRIP2 was independent of the catalytic activity of ADAM. Therefore, we transformed WT-N and deletion mutants into yeast cells and compared CRIP2 binding ability by 3AT-assay (Fig. 1B). The degree of binding was decreased in the WT-NΔDI and WT-NΔCys mutants, but not in the WT-NΔEGF mutant. Binding was also decreased with WT-MP and the control pAS vector. These results indicate that CRIP2 recognizes the DI and Cys domains of ADAM19 for its binding.

3.2. Interaction between ADAM19 and CRIP2 in COS-7 cells

To investigate the interaction between CRIP2 and ADAM19 in mammalian cells, we performed co-immunoprecipitation experiments. Myc–CRIP2 and ADAM19–V5 were overexpressed in COS-7 cells. When ADAM19–V5 was immunoprecipitated with anti-V5 antibody (Fig. 2B), Myc–CRIP2 was co-precipitated (Fig. 2A), indicating that CRIP2 was associated with ADAM19.

CRIP2 is widely expressed, with highest expression in the heart and moderate expression in the lungs, placenta, and kidneys [7]. ADAM19 is also ubiquitously expressed and is especially high in the heart, lungs, and bone [8]. These comparable expression patterns suggest a physiological role of CRIP2 binding to ADAM19.

3.3. ADAM19 promotes the secretion of CRIP2

CRIP2 does not have an apparent transmembrane domain or signal sequence, although CRIP2 was identified as the endothelial receptor for a heart-targeting peptide [9]. Moreover, it was reported that CRIP2 is enriched in the submembranous cell cortex and is a binding partner of submembranous protein tyrosine phosphatase, PTP-BL [10], indicating that CRIP2 is expressed at the cell surface. An analysis of the CRIP2 sequence using SecretomeP, http://www.cbs.dtu.dk/services/SecretomeP/, an algorithm capable of predicting the presence or absence of both classical and non-classical signal sequences, revealed that CRIP2 is a non-classical secretable protein, without a classical signal sequence. Consistent with previous reports, CRIP2 was observed on the cell surface in HA–CRIP2-overexpressing A172 cells (Fig. 3A). We investigated the secretion of CRIP2 and the influence of ADAM19 on secretion levels in H4 cells stably overexpressing ADAM19–V5 or a control vector. These cells were transfected with HA–CRIP2, and the

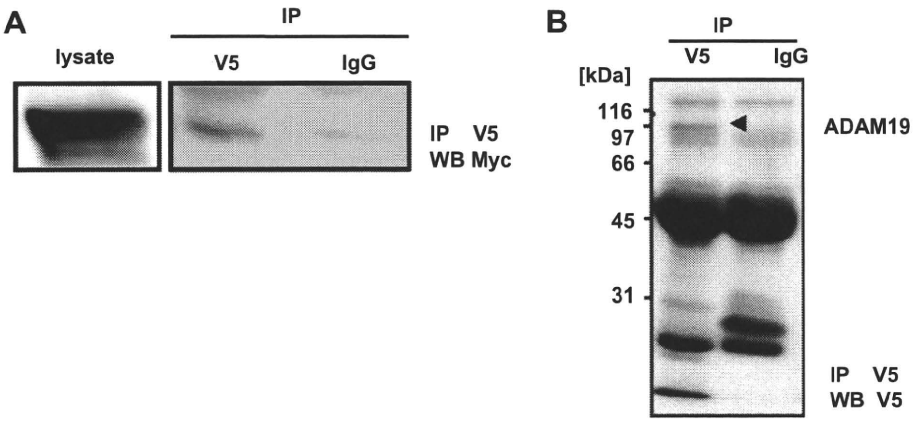

Fig. 2. Interaction between ADAM19 and CRIP2 in COS-7 cells. (A) COS-7 cells overexpressing ADAM19–V5 and Myc–CRIP2 were immunoprecipitated with anti-V5 antibody and anti-mouse IgG, followed by Western blot analysis of the IP fraction using anti-Myc antibody. The expression level of Myc–CRIP2 was confirmed in the lysate fraction. (B) ADAM19–V5 was immunoprecipitated with anti-V5 antibody. Some nonspecific binding was observed in the IgG lane, but the amounts of immunoprecipitated ADAM19–V5 and co-precipitated Myc–CRIP2 were comparable.

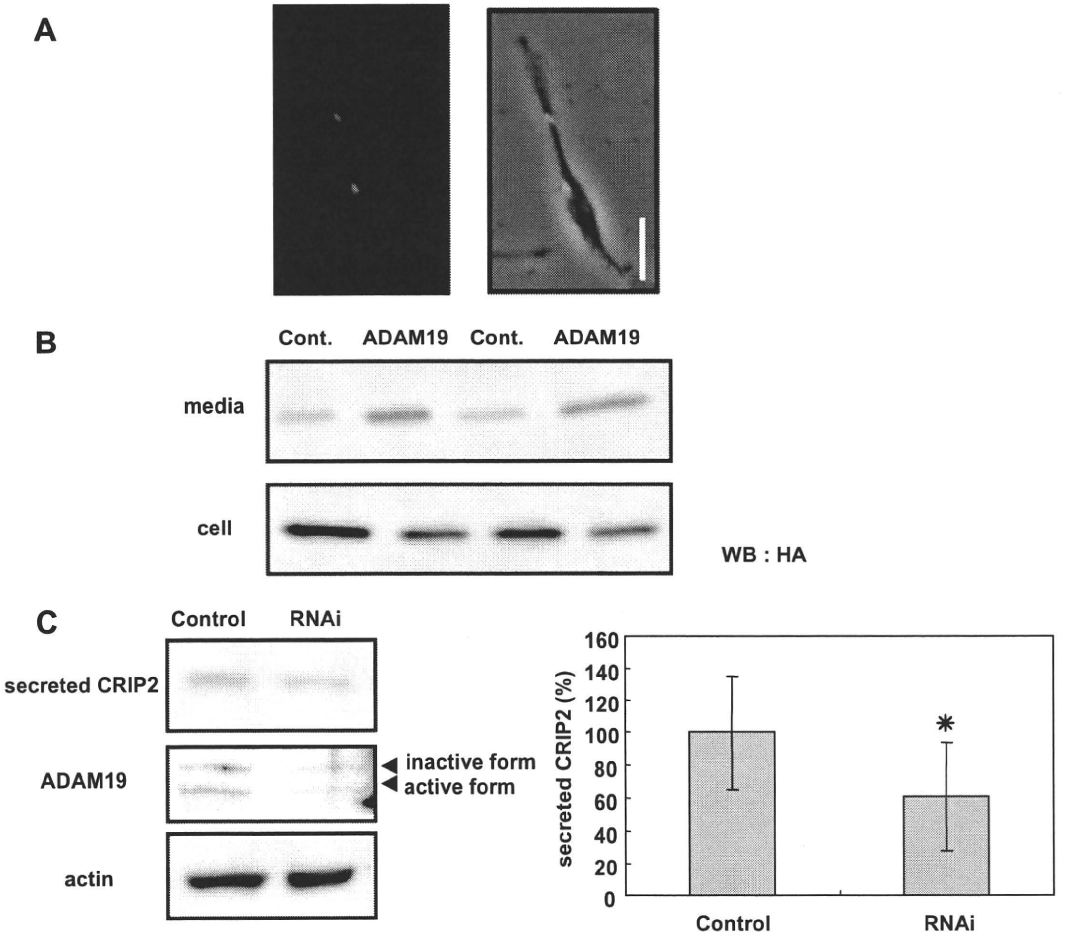

Fig. 3. ADAM19 promotes the secretion of CRIP2. (A) A172 cells overexpressing HA–CRIP2 were immunostained with anti-HA antibody and Alexa 488-conjugated secondary antibody without membrane permeabilization. CRIP2 was observed on the cell surface (scale bar, 20 μm). (B) The amounts of secreted CRIP2 in the medium and intracellular CRIP2 were compared by immunoblotting with anti-HA antibody. The amount of secreted CRIP2 was increased and the intracellular level of CRIP2 was decreased in H4 cells stably overexpressing ADAM19–V5, compared with the control. (C) A172 cells were transfected with 100 nM negative-control RNA (Control) or stealth RNA (RNAi). Following incubation for 4 h, the medium was collected, and the secreted CRIP2 content was determined by Western blot analysis with anti-CRIP2 antibody (upper panel and right graph). The suppression of ADAM19 expression was confirmed on Western blots of cell lysates using anti-ADAM19 antibody (middle panel). The membrane was stripped and then incubated with anti-actin antibody. Values represent the means ± SD of three experiments. Statistical analysis was performed by the one-tailed Student's *t*-test, with a value of $p = 0.03$ considered significant (right graph).

secreted and intracellular levels of HA–CRIP2 were compared by immunoblotting with HA antibody (Fig. 3B). The secretion of CRIP2 was increased with a concomitant decrease in the intracellular level of CRIP2 in ADAM19-overexpressing cells compared with

control cells. When ADAM19 expression was inhibited with RNAi in A172 cells (Fig. 3C), the amount of secreted CRIP2 was decreased by 40%, based on quantitative immunoblot analysis with CRIP2 antibody. The results demonstrate that CRIP2 secretion is reduced in the absence of ADAM19 and promoted in the presence of ADAM19, through a non-classical secretory pathway.

3.4. Activation of ADAM19 and promotion of CRIP2 secretion by LPS treatment

CRIP2 has two LIM domains with a cysteine-rich zinc-finger motif. LIM domains, C-X_2-C-X_{16-23}-H-X_2-C-X_2-C-X_2-C-X_{16-21}-C-X_{2-3}-C/H/D, are present in a variety of proteins with diverse functions and subcellular distributions; these include transcription factors, proto-oncogene products, and components of adhesion plaques and the actin-based cytoskeleton [11,12]. LIM-domain proteins have been implicated in development, cell regulation, and cell structure, and are divided into two classes based on the presence or absence of DNA-binding homeodomains. CRIP2 is in the subfamily that lacks homeodomains; this group consists of CRIP, CRIP2, TLP-A, and TLP-B [7,13]. When treated with LPS, CRIP-overexpressing transgenic mice showed an altered cytokine pattern, with increases in interleukin (IL)-6 and IL-10 production and decreased interferon-γ (IFN-γ), which suggests a LPS-related shift in favor of T helper 2 (Th2) over Th1 cytokines and indicates that CRIP regulates the expression/secretion of the cytokines [14]. We used immunoblotting to examine the effect of LPS on CRIP2 secretion by A172 cells treated with 0.1 μg/mL LPS for 4 h (Fig. 4A). The LPS-treated A172 cells released 1.4 times the CRIP2 secreted by DMSO-treated control cells. Moreover, the active form of ADAM19 was decreased and the processed C-fragment of ADAM19, representing the secreted form, was increased, compared with the levels in non-LPS-treated cells (Fig. 4B). Thus, LPS treatment activated ADAM19 autolysis, thereby producing the secreted form of ADAM19, which enhanced CRIP2 secretion.

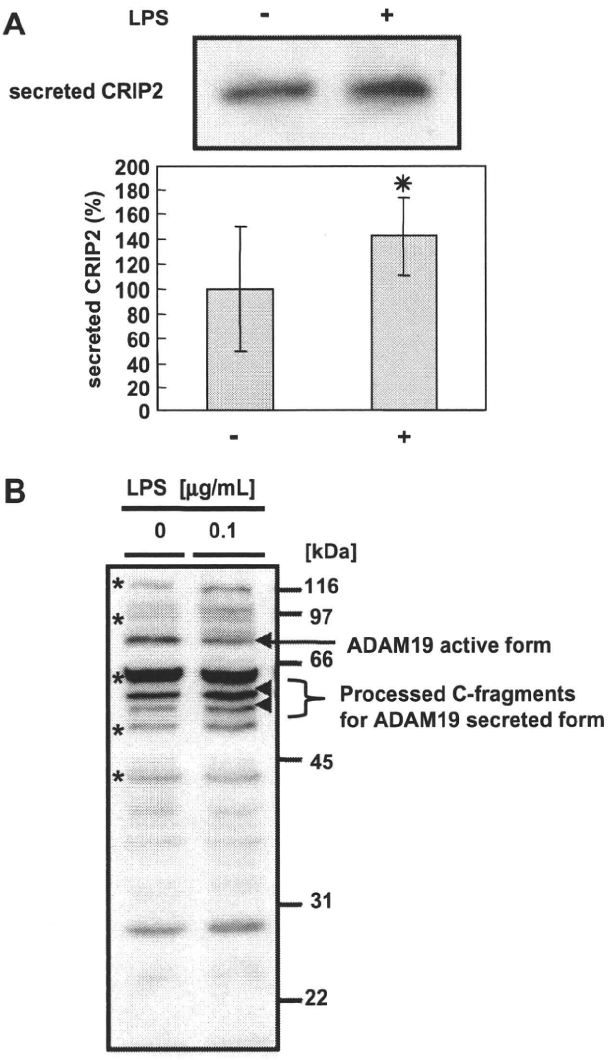

Fig. 4. Activation of ADAM19 and promotion of CRIP2 secretion by LPS treatment. (A) A172 cells were treated with or without 0.1 μg/mL LPS in serum-free DMEM for 4 h. All samples contained 0.1% DMSO. The medium was collected, and the secreted CRIP2 content was determined by Western blot analysis with anti-CRIP2 antibody. Values represent the means ± SD of three experiments. Statistical analysis was performed by the one-tailed Student's *t*-test, with a value of $p = 0.03$ considered significant. (B) The ADAM19 protein level in A172 cells treated with or without LPS was analyzed with anti-ADAM19 antibody. Asterisks indicate nonspecific bands.

4. Discussion

In this study, we identified CRIP2 as a novel binding protein of ADAM19 through its DI and Cys domains (Fig. 1). The DI domain of ADAM can interact with multiple integrins, and the interactions influence cell adhesion and cell–cell interactions [15]. The Cys domain of ADAM12 is the association site of syndecan and is related to integrin-dependent cell spreading [16]. In addition to cell adhesion and cell migration, DI and Cys can influence the proteolytic function of ADAM. It has been reported that DI and Cys domains play active roles in regulating ADAM13 protease function *in vivo* [17], and that the Cys domain of ADAM10 helps the specific recognition of the Ephrin ligand and Eph receptor complex [18]. We had hypothesized that CRIP2 has a role in regulating ADAM19 activity in APP processing. However, we detected no influence of CRIP2 on the α-secretase activity of ADAM19 (data not shown). Nevertheless, it is possible that CRIP2 regulates the proteolysis of other substrates by ADAM19. ADAM19 is associated with the proteolytic processing of neuregulin [19] and TNF-related activation-induced cytokine (TRANCE) [20]. ADAM19 is expressed mainly in the heart and nervous system during development and participates in the proteolytic processing of β-type neuregulin (NRG β1), which is involved in the differentiation of those cells [21]. In cardiac neural crest cells, ADAM19 plays a critical role in the formation of the ventricular septum [22], which was abnormal in ADAM19$^{-/-}$ mice. Interestingly, it has been reported that CRIP2 is associated with the development of cardiac neural crest cells in zebrafish [23]. It is possible that CRIP2 is associated with ADAM19 in cardiac neural crest cells and is related to heart development.

We showed that CRIP2 is a secretable protein without a classical signal. The secretion of CRIP2 was upregulated by ADAM19 expression and downregulated by RNAi-mediated inhibition of ADAM19 expression (Fig. 3). These results indicate that ADAM19 promotes the secretion of CRIP2 through a non-classical secretory pathway. Moreover, CRIP2 secretion was increased in parallel with the LPS-stimulated autolytic processing of ADAM19 (Fig. 4). Therefore, we suggest that ADAM19 autolysis is activated by LPS and promotes the secretion of CRIP2. In the present study, CRIP2 secretion was increased in response to the extracellular cytotoxin LPS. The function of secreted CRIP2 remains to be elucidated. It is possible that CRIP2 functions as a cytokine, or that it activates Th2 cytokines, as well as CRIP. Pro-inflammatory Th1 and anti-inflammatory Th2 responses are mutually inhibitory. In addition, non-steroidal anti-inflammatory drugs (NSAIDs) have a protective function against the development of AD [24]. Furthermore, it has been reported that Wnt3a regulates the development of cardiac neural crest cells in zebrafish by modulating the expression of CRIP2

[23], and that the Wnt/β-catenin signaling pathway plays an important role in neuroprotection against Aβ neurotoxicity [25,26]. Therefore, it is possible that secreted CRIP2 has a neuroprotective role. Further studies are necessary to explore this hypothesis.

In conclusion, we identified CRIP2 as a novel binding protein of ADAM19 and that it recognizes the DI and Cys domains of ADAM19. Furthermore, we clarified that CRIP2 is a secretable protein without a classical signal sequence and demonstrated that CRIP2 secretion was increased by ADAM19 upon LPS stimulation. Thus, LPS treatment promotes ADAM19 autolysis and the non-classical secretion of CRIP2.

Acknowledgments

We thank Dr. Hiroshi Ishiguro (Carna Bioscience, Inc.) for providing hADAM19 cDNA and Dr. Daikichi Fukushima (ONO Pharmaceutical Co., Ltd.) for providing A172 glioblastoma cells. This work was supported by a grant from the Ministry of Education, Science, Sports, Culture, and Technology of Japan.

References

[1] T. Kang, Y.G. Zhao, D. Pei, J.F. Sucic, Q.X. Sang, Intracellular activation of human adamalysin 19/disintegrin and metalloproteinase 19 by furin occurs via one of the two consecutive recognition sites, J. Biol. Chem. 277 (2002) 25583–25591.
[2] A.P. Huovila, A.J. Turner, M. Pelto-Huikko, I. Karkkainen, R.M. Ortiz, Shedding light on ADAM metalloproteinases, Trends Biochem. Sci. 30 (2005) 413–422.
[3] D.R. Edwards, M.M. Handsley, C.J. Pennington, The ADAM metalloproteinases, Mol. Aspects Med. 29 (2008) 258–289.
[4] J.A. Hardy, G.A. Higgins, Alzheimer's disease: the amyloid cascade hypothesis, Science 256 (1992) 184–185.
[5] C. Tanabe, N. Hotoda, N. Sasagawa, A. Sehara-Fujisawa, K. Maruyama, S. Ishiura, ADAM19 is tightly associated with constitutive Alzheimer's disease APP alpha-secretase in A172 cells, Biochem. Biophys. Res. Commun. 352 (2007) 111–117.
[6] T. Kang, H.I. Park, Y. Suh, Y.G. Zhao, H. Tschesche, Q.X. Sang, Autolytic processing at Glu586-Ser587 within the cysteine-rich domain of human adamalysin 19/disintegrin-metalloproteinase 19 is necessary for its proteolytic activity, J. Biol. Chem. 277 (2002) 48514–48522.
[7] M.A. Karim, K. Ohta, M. Egashira, Y. Jinno, N. Niikawa, I. Matsuda, Y. Indo, Human ESP1/CRP2, a member of the LIM domain protein family: characterization of the cDNA and assignment of the gene locus to chromosome 14q32.3, Genomics 31 (1996) 167–176.
[8] P. Wei, Y.G. Zhao, L. Zhuang, S. Ruben, Q.X. Sang, Expression and enzymatic activity of human disintegrin and metalloproteinase ADAM19/meltrin beta, Biochem. Biophys. Res. Commun. 280 (2001) 744–755.
[9] L. Zhang, J.A. Hoffman, E. Ruoslahti, Molecular profiling of heart endothelial cells, Circulation 112 (2005) 1601–1611.
[10] M. van Ham, H. Croes, J. Schepens, J. Fransen, B. Wieringa, W. Hendriks, Cloning and characterization of mCRIP2, a mouse LIM-only protein that interacts with PDZ domain IV of PTP-BL, Genes Cells 8 (2003) 631–644.
[11] X. Wang, G. Lee, S.A. Liebhaber, N.E. Cooke, Human cysteine-rich protein. A member of the LIM/double-finger family displaying coordinate serum induction with c-myc, J. Biol. Chem. 267 (1992) 9176–9184.
[12] I. Sadler, A.W. Crawford, J.W. Michelsen, M.C. Beckerle, Zyxin and cCRP: two interactive LIM domain proteins associated with the cytoskeleton, J. Cell Biol. 119 (1992) 1573–1587.
[13] J. Kirchner, K.A. Forbush, M.J. Bevan, Identification and characterization of thymus LIM protein: targeted disruption reduces thymus cellularity, Mol. Cell Biol. 21 (2001) 8592–8604.
[14] L. Lanningham-Foster, C.L. Green, B. Langkamp-Henken, B.A. Davis, K.T. Nguyen, B.S. Bender, R.J. Cousins, Overexpression of CRIP in transgenic mice alters cytokine patterns and the immune response, Am. J. Physiol. Endocrinol. Metab. 282 (2002) E1197–E1203.
[15] M. Tomczuk, Y. Takahashi, J. Huang, S. Murase, M. Mistretta, E. Klaffky, A. Sutherland, L. Bolling, S. Coonrod, C. Marcinkiewicz, D. Sheppard, M.A. Stepp, J.M. White, Role of multiple beta1 integrins in cell adhesion to the disintegrin domains of ADAMs 2 and 3, Exp. Cell Res. 290 (2003) 68–81.
[16] K. Iba, R. Albrechtsen, B. Gilpin, C. Frohlich, F. Loechel, A. Zolkiewska, K. Ishiguro, T. Kojima, W. Liu, J.K. Langford, R.D. Sanderson, C. Brakebusch, R. Fassler, U.M. Wewer, The cysteine-rich domain of human ADAM 12 supports cell adhesion through syndecans and triggers signaling events that lead to beta1 integrin-dependent cell spreading, J. Cell Biol. 149 (2000) 1143–1156.
[17] K.M. Smith, A. Gaultier, H. Cousin, D. Alfandari, J.M. White, D.W. DeSimone, The cysteine-rich domain regulates ADAM protease function in vivo, J. Cell Biol. 159 (2002) 893–902.
[18] P.W. Janes, N. Saha, W.A. Barton, M.V. Kolev, S.H. Wimmer-Kleikamp, E. Nievergall, C.P. Blobel, J.P. Himanen, M. Lackmann, D.B. Nikolov, Adam meets Eph: an ADAM substrate recognition module acts as a molecular switch for ephrin cleavage in trans, Cell 123 (2005) 291–304.
[19] K. Shirakabe, S. Wakatsuki, T. Kurisaki, A. Fujisawa-Sehara, Roles of Meltrin beta /ADAM19 in the processing of neuregulin, J. Biol. Chem. 276 (2001) 9352–9358.
[20] V. Chesneau, J.D. Becherer, Y. Zheng, H. Erdjument-Bromage, P. Tempst, C.P. Blobel, Catalytic properties of ADAM19, J. Biol. Chem. 278 (2003) 22331–22340.
[21] K. Kurohara, K. Komatsu, T. Kurisaki, A. Masuda, N. Irie, M. Asano, K. Sudo, Y. Nabeshima, Y. Iwakura, A. Sehara-Fujisawa, Essential roles of Meltrin beta (ADAM19) in heart development, Dev. Biol. 267 (2004) 14–28.
[22] K. Komatsu, S. Wakatsuki, S. Yamada, K. Yamamura, J. Miyazaki, A. Sehara-Fujisawa, Meltrin beta expressed in cardiac neural crest cells is required for ventricular septum formation of the heart, Dev. Biol. 303 (2007) 82–92.
[23] X. Sun, R. Zhang, X. Lin, X. Xu, Wnt3a regulates the development of cardiac neural crest cells by modulating expression of cysteine-rich intestinal protein 2 in rhombomere 6, Circ. Res. 102 (2008) 831–839.
[24] P.L. McGeer, M. Schulzer, E.G. McGeer, Arthritis and anti-inflammatory agents as possible protective factors for Alzheimer's disease: a review of 17 epidemiologic studies, Neurology 47 (1996) 425–432.
[25] L. Baum, L. Hansen, E. Masliah, T. Saitoh, Glycogen synthase kinase 3 alteration in Alzheimer disease is related to neurofibrillary tangle formation, Mol. Chem. Neuropathol. 29 (1996) 253–261.
[26] A.R. Alvarez, J.A. Godoy, K. Mullendorff, G.H. Olivares, M. Bronfman, N.C. Inestrosa, Wnt-3a overcomes beta-amyloid toxicity in rat hippocampal neurons, Exp. Cell Res. 297 (2004) 186–196.

Journal of Neuroscience Research

Journal of Neuroscience Research 88:3588–3597 (2010)

Efficient Four-Drug Cocktail Therapy Targeting Amyloid-β Peptide for Alzheimer's Disease

Masashi Asai,[1,2]* Nobuhisa Iwata,[2] Taisuke Tomita,[3,4] Takeshi Iwatsubo,[3,4,5] Shoichi Ishiura,[6] Takaomi C. Saido,[2] and Kei Maruyama[1]

[1]Department of Pharmacology, Faculty of Medicine, Saitama Medical University, Saitama, Japan
[2]Laboratory for Proteolytic Neuroscience, RIKEN Brain Science Institute, Saitama, Japan
[3]Department of Neuropathology and Neuroscience, Graduate School of Pharmaceutical Sciences, The University of Tokyo, Tokyo, Japan
[4]Core Research for Evolutional Science and Technology (CREST), Japan Science and Technology Corporation, Tokyo, Japan
[5]Department of Neuropathology, Graduate School of Medicine, The University of Tokyo, Tokyo, Japan
[6]Department of Life Sciences, Graduate School of Arts and Sciences, The University of Tokyo, Tokyo, Japan

Cocktail treatment is an effective multidrug medication therapy for some diseases, such as cancer and AIDS, because of the additive or synergistic effect of each medicine and relief from adverse effects. Amyloid-β peptide (Aβ), which is now recognized as central to the development of Alzheimer's disease (AD), is derived from the sequential proteolysis of amyloid precursor protein (APP) by β- and γ-secretases. Secretase inhibitors are one of most attractive targets for therapeutic intervention in AD. However, because β- and γ-secretases cleave not only APP but also other substrate proteins, strong inhibition of these secretases leads to severe adverse effects. Some nonsteroidal antiinflammatory drugs (NSAIDs) and cholesterol-lowering drugs (statins) can modify the production of Aβ. Here, we report that a cocktail treatment with four drugs (NSAID, statin, and β- and γ-secretase inhibitors) had additive effects on the reduction of Aβ levels in cultured cells without competing with each other. Moreover, the four-drug cocktail treatment caused no changes in processing of the γ-secretase substrate Notch. This is suggests that this cocktail treatment could be a new therapeutic approach for AD.

Key words: NSAID; β-secretase inhibitor; γ-secretase inhibitor; statin; cocktail therapy

Alzheimer's disease (AD) is the most frequent type of elderly dementia. It is characterized by the deposition of amyloid plaques, accumulation of neurofibrillary tangles, and loss of neurons and synapses in particular areas of the brain (Selkoe, 2002; Mattson, 2004). AD occurs in both sporadic and familial forms, with generally similar pathology according to the amyloid hypothesis, which is based on the metabolic imbalance between the production and clearance of amyloid-β peptide (Aβ; Iwata et al., 2005; Blennow et al., 2006). Aβ is derived from the sequential proteolysis of amyloid precursor protein (APP) by β- and γ-secretases (Mattson, 2004; Blennow et al., 2006) and plays a critical role in AD pathogenesis. Therefore, lowering Aβ levels in the brain serves as a disease-modifying therapy for AD.

Because inhibitors of β- and γ-secretases directly block Aβ production, they are promising and attractive therapeutic targets for AD (Mattson, 2004; Marks and Berg, 2008). Indeed, many compounds have been developed that inhibit these secretases and reduce Aβ levels in vitro and in vivo (Stachel et al., 2004; Wong et al. 2004; Asai et al., 2006). However, because β- and γ-secretases act on a variety of substrates, type I membrane proteins, in addition to APP (Marks and Berg, 2008), it has been suggested that strong inhibition of their protease activity may produce adverse effects (De Strooper et al., 1999; Geling et al., 2002; Wong et al., 2004; Dominguez et al., 2005; Willem et al., 2006).

Some nonsteroidal antiinflammatory drugs (NSAIDs) and widely used cholesterol-lowering drugs (statins) are also capable of reducing Aβ levels (Fassbender et al., 2001; Weggen et al., 2001; Eriksen et al., 2003). Statins, 3-hydroxy-3-methylglutaryl-CoA (HMG-CoA) reductase inhibitors, suppress Aβ production and activate the alter-

Contract grant sponsor: Grant-in-Aid for Young Scientists (19790194) from Japan Society for the Promotion of Science (JSPS) (to M.A.); Contract grant sponsor: Grant-in-Aid for Scientific Research (20590260) from Japan Society for the Promotion of Science (JSPS) (to K.M.); Contract grant sponsor: Ochiai Memorial Award 2004 (to M.A.).

*Correspondence to: Masashi Asai, 38 Moro-hongo, Moroyama-machi, Iruma-gun, Saitama 350-0495, Japan. E-mail: asai@saitama-med.ac.jp

Received 20 January 2010; Revised 13 July 2010; Accepted 1 August 2010

Published online 1 October 2010 in Wiley Online Library (wileyonlinelibrary.com). DOI: 10.1002/jnr.22503

nate pathway for APP metabolism, the nonamyloidogenic α-secretase pathway (Fassbender et al., 2001). Several NSAIDs, including sulindac sulfide, modulate γ-secretase activity, thereby decreasing the secretion of Aβ42, which is more prone to aggregation than Aβ40 and is predominantly deposited in AD brains, but show little effect on the secretion of Aβ40 (Weggen et al., 2001). Almost all familial AD-linked mutations of causal genes, such as APP and presenilin (PS) 1 and 2, promote the production of Aβ42 and elevate the Aβ42-to-Aβ40 ratio (Aβ42/Aβ40), accelerating AD pathogenesis (Wolfe, 2007). Thus, NSAIDs are potential disease-modifying agents for AD, although a relatively high dose is required for this effect (Blennow et al., 2006; Weggen et al., 2007).

Although the removal of Aβ from the brain is required for treatment of AD, there are, currently, no fundamental therapeutic drugs targeting Aβ (Saido and Iwata, 2006; Marks and Berg, 2008). Indeed, the sole use of secretase inhibitors at a high dose is likely to cause adverse effects. However, a cocktail treatment (a combination of 2–4 drugs) at relatively low doses (e.g., 20–30% efficacies in each case) would give rise to an additive or synergistic effect and alleviate the adverse effects (Saido and Iwata, 2006). There is much evidence suggesting that there are multiple strategies to reduce Aβ levels, so we designed a combinatorial approach targeting different processes in the production of Aβ. Inhibition of Aβ production prevents AD development via formation of particular forms of Aβ, such as Aβ oligomers. The drug cocktail consisted of β- and γ-secretase inhibitors, an NSAID, and a statin. Here, we report that this four-drug cocktail was remarkably effective in reducing Aβ levels without competing with each other or causing apparent adverse effects. It is suggested that this four-drug cocktail is a new and potentially powerful approach to the treatment of AD.

MATERIALS AND METHODS

Reagents and Antibodies

The β-secretase inhibitor IV (*N*-[(1*S*, 2*R*)-1-benzyl-3-(cyclopropylamino)-2-hydroxypropyl]-5-[methyl(methylsulfonyl)amino-*N'*-[(1*R*)-1-phenylethyl]isophthalamide; Stachel et al., 2004), γ-secretase inhibitor XXI (also known as "compound E"; (*S,S*)-2-[2-(3,5-difluorophenyl)-acetylamino]-*N*-(1-methyl-2-oxo-5-phenyl-2,3-dihydro-1H-benzo[e][1,4]diazepin-3-yl)-propionamide; Seiffert et al., 2000), and the sodium salt of simvastatin were purchased from Merck KGaA (Darmstadt, Germany); sulindac sulfide was purchased from Sigma-Aldrich (St. Louis, MO). All drugs were dissolved in sterilized dimethyl sulfoxide (DMSO) and added to cell culture medium to give a final concentration of 0.1% DMSO. Monoclonal antibody 22C11 (Chemicon, Temecula, CA), which recognizes amino acid residues 66–81 at the N-terminus of APP, was used at a concentration of 1:1,000. Monoclonal antibody 2B3 (Immuno-Biological Laboratories Co., Gunma, Japan), which recognizes amino acid residues at the C-terminal end of human soluble extracellular fragment of APP generated by α-secretase (sAPPα), was used at a concentration of 2 μg/ml. The polyclonal anti-sAPPβ$_{NL}$ antibody was used at a concentration of 1:1,000 to detect the soluble extracellular fragment of APPsw (APP with Swedish mutation) generated by β-secretase (sAPPβ), as previously described (Asai et al., 2007). Monoclonal antibody 82E1 (Immuno-Biological Laboratories Co.), which recognizes amino acid residues 1–16 of the human Aβ sequence, was used at 1 μg/ml. Polyclonal anti-APP antibody (catalogue No. A8717; Sigma-Aldrich), which recognizes amino acid residues 676–695 at the C-terminus of APP$_{695}$, was used at a concentration of 1:15,000. Monoclonal antibody AC-74 (Sigma-Aldrich), which recognizes amino acid residues at the N-terminal end of β-actin, was used at a concentration of 1:5,000. Monoclonal antibody 9B11 (Cell Signaling Technology, Danvers, MA), which recognizes the myc epitope tag (corresponding to amino acid residues 410–419 of human c-Myc), was used at a concentration of 1:1,000.

Cell Culture

An expression vector encoding mouse Notch deleted extracellular domain (mNotch$^{\Delta E}$) in pCS2 (Kopan et al., 1996) was provided by Dr. Raphael Kopan (Washington University). An expression vector encoding enhanced green fluorescent protein (EGFP) was digested from pEGFP-N1 (BD Biosciences Clontech Laboratories, Palo Alto, CA) and subcloned into the pcDNA3 vector (Invitrogen, Carlsbad, CA; Imamura et al., 2009). A stable Neuro2a (N2a) cell line (mNotch$^{\Delta E}$-N2a cells) doubly expressing mNotch$^{\Delta E}$ and EGFP and a stable H4 cell line (APP$_{NL}$-H4 cells) stably expressing human APP$_{695}$ with the Swedish mutation (Asai et al, 2007) were cultured in Dulbecco's modified Eagle's medium (DMEM; Invitrogen) at 37°C in 5% CO_2. DMEM was supplemented with 10% fetal bovine serum (BioWest, Nuaillé, France), 100 U/ml penicillin, 100 μg/ml streptomycin (Invitrogen), and 160 μg/ml G418 (Merck KGaA) for mNotch$^{\Delta E}$-N2a cells or 150 μg/ml hygromycin B (Wako Pure Chemical Industries Ltd., Osaka, Japan) for APP$_{NL}$-H4 cells. Cells were grown for 24 hr in a 24-well plate or a 6-cm dish. The drugs were then added to the conditioned culture medium, and the cells were incubated for 24 hr. Both conditioned media were supplemented with lipid-free serum (BioWest).

Cell Toxicity Analysis

Cell toxicity assay was assessed with a cytotoxicity detection kit (Roche Diagnostics GmbH, Mannheim, Germany) that determines the amount of lactate dehydrogenase (LDH) released into the cell culture medium from dying cells.

Aβ Sandwich ELISA

Extracellular Aβ40 and Aβ42 levels in the conditioned media from cultured mNotch$^{\Delta E}$-N2a or APP$_{NL}$-H4cells were measured by an Aβ enzyme-linked immunosorbent assay (ELISA) kit (Wako Pure Chemical Industries Ltd.).

Western Blot Analysis

Cells treated with drugs were harvested and lysed in a buffer containing 10 mM HEPES (pH 7.4), 150 mM NaCl, 0.5% Triton X-100, and protease inhibitor cocktail (Roche

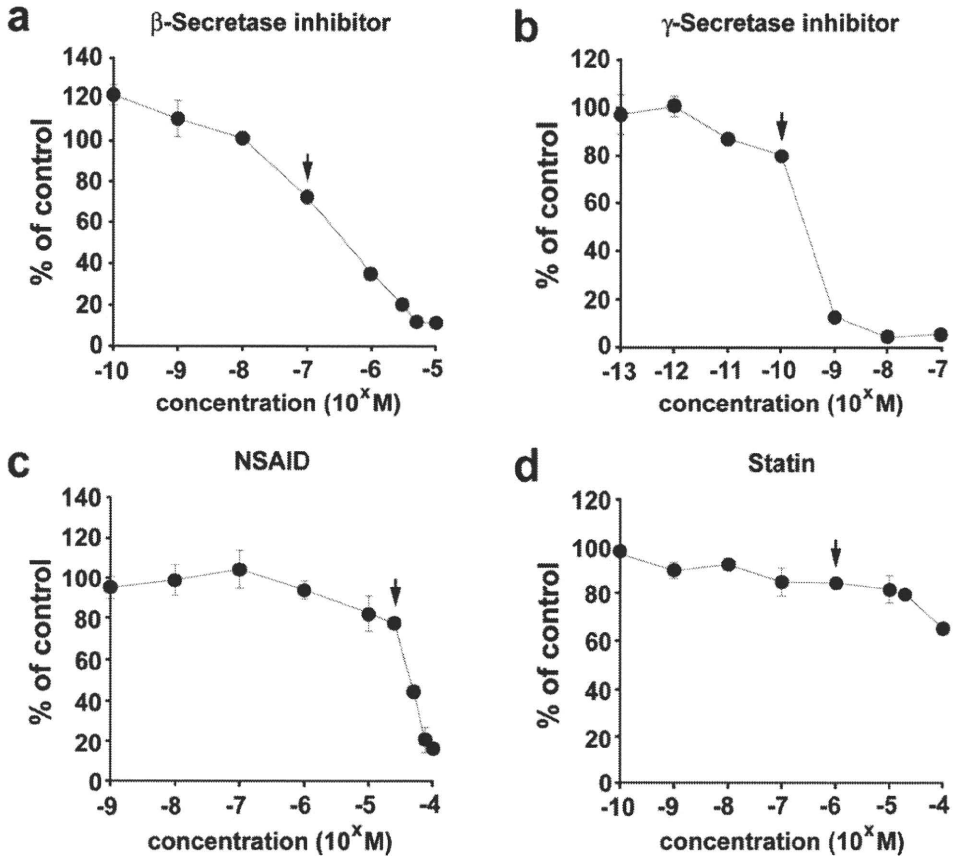

Fig. 1. Determination of the concentration of each single drug for the cocktail treatment. Amount of Aβ42 released into the conditioned medium from APP_{NL}-H4 cells treated with each drug was measured by sandwich ELISA β-secretase inhibitor (**a**), γ-secretase inhibitor (**b**), NSAID (**c**), and statin (**d**). Data represent the mean ± SD of three experiments. Actual values of Aβ40 and Aβ42 concentrations in the control group (vehicle treatment) are 1,861 ± 168 pM and 58.3 ± 7.2 pM, respectively. Each arrow indicates the concentrations for which the combinational drug experiments shown in Figures 2–5 were performed.

Applied Science) on ice. The cell lysate was freeze-thawed three times at 20-min intervals and centrifuged at 13,000*g* for 15 min at 4°C. The supernatant protein concentrations were determined using a BCA protein assay kit (Pierce Biotechnology, Rockford, IL).

sAPP secreted into the conditioned media was precipitated with heparin agarose resin (Pierce Biotechnology). Equal amounts of proteins in the cell lysates or sAPP collected from equal volumes of conditioned media were subjected to sodium dodecyl sulfate-polyacrylamide gel electrophoresis, and the proteins in the gels were transferred to polyvinylidene difluoride membranes (Hybond-P; GE Healthcare UK, Buckinghamshire, United Kingdom) or nitrocellulose transfer membrane (Protran; Whatman GmbH, Dassel, Germany). The membranes were probed with an appropriate primary antibody and then treated with an appropriate secondary antibody, namely, horseradish peroxidase-conjugated anti-mouse or anti-rabbit IgG (GE Healthcare UK). The protein bands were visualized using an enhanced chemiluminescence (ECL) detection method (GE Healthcare UK), and band intensity was analyzed with a densitometer (LAS-4000; Fujifilm Corporation, Tokyo, Japan), using the Science Laboratory 2001 Image Gauge software (Fujifilm Corporation).

Statistical Analysis

All values were expressed as the mean ± SD. For comparisons of two groups, a two-tailed Student's *t*-test was used. For comparisons among more than three groups, Dunnett's or SNK multiple-comparisons tests were used. A difference was considered significant at $P < 0.05$.

RESULTS

Determination of Single Doses of Drugs

We selected the most potent compounds for the β- and γ-secretase inhibitors, NSAID, and statin from commercially available reagents; we used the β-secretase inhibitor IV (Stachel et al., 2004), γ-secretase inhibitor XXI/compound E (Seiffert et al., 2000), sulindac sulfide (Weggen et al., 2001), and simvastatin (Fassbender et al., 2001). We first evaluated the inhibitory effect of each drug on Aβ42 production (Fig. 1). All of these drugs inhibited production of Aβ42, whose secretion from APP_{NL}-H4 cells was decreased in a dose-dependent manner. On the basis of these results, we selected a dose for each drug with an approximately 15–30% inhibitory

effect on Aβ42 production: β-secretase inhibitor, 100 nM (% of inhibition on Aβ42 production = 27.7%); γ-secretase inhibitor, 100 pM (19.5%); NSAID, 25 μM (23%); and statin, 1 μM (15.5%); as indicated by the arrows in Figure 1. We also confirmed that these doses had no significant effect on LDH release compared with the vehicle treatment (Table I).

TABLE I. Effect of Single Drug or Cocktail Administration on Cell Toxicity*

Reagent	LDH release (% of control)
Vehicle	100.0 ± 3.7
β-Secretase inhibitor	90.9 ± 6.4
γ-Secretase inhibitor	92.2 ± 6.8
NSAID	92.2 ± 5.0
Statin	105.0 ± 8.1
Cocktail	109.1 ± 13.4

*APP_{NL}-H4 cells were treated with the indicated reagent for 24 hr, and cell toxicity was assessed by the LDH assay. Data are the mean ± SD of nine experiments in each group.

Combinatorial Effects of the β-Secretase Inhibitor With One of the Other Drugs on Aβ Production

We next examined both Aβ40 and Aβ42 levels in the conditioned media from APP_{NL}-H4 cells treated with the γ-secretase inhibitor, NSAID, or statin, in the presence of the β-secretase inhibitor (Fig. 2). The administration of each drug in combination with the β-secretase inhibitor significantly reduced Aβ40 levels at low doses of the β-secretase inhibitor compared with administration of the β-secretase inhibitor alone (Fig. 2a). However, at a high concentration of the β-secretase inhibitor, a significant cooperative effect on Aβ40 levels was not observed (Fig. 2a). The β-secretase inhibitor showed a significant reduction in Aβ42 levels only at doses of 10^{-9} and 10^{-8} M in combination with the γ-secretase inhibitor, whereas the NSAID and statin

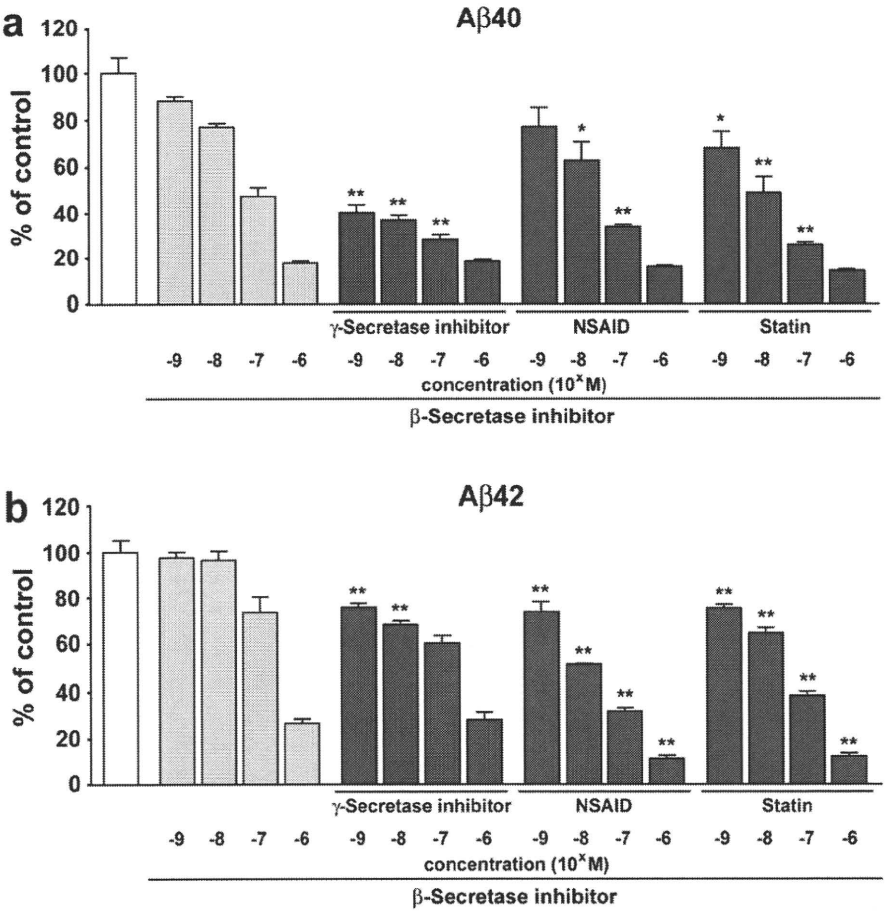

Fig. 2. Effect of the combination of the β-secretase inhibitor with the other drugs on Aβ40 and Aβ42 levels. Amount of Aβ released into the conditioned medium from APP_{NL}-H4 cells treated with each drug in the presence of the β-secretase inhibitor was measured by sandwich ELISA. Doses of the γ-secretase inhibitor, NSAID, and statin were 100 pM, 25 μM, and 1 μM, respectively. Levels of Aβ are expressed as Aβ40 (**a**) and Aβ42 (**b**). Data represent the mean ± SD of three experiments. *$P < 0.05$, **$P < 0.01$, significantly different from the group treated with the β-secretase inhibitor alone at the corresponding concentration.

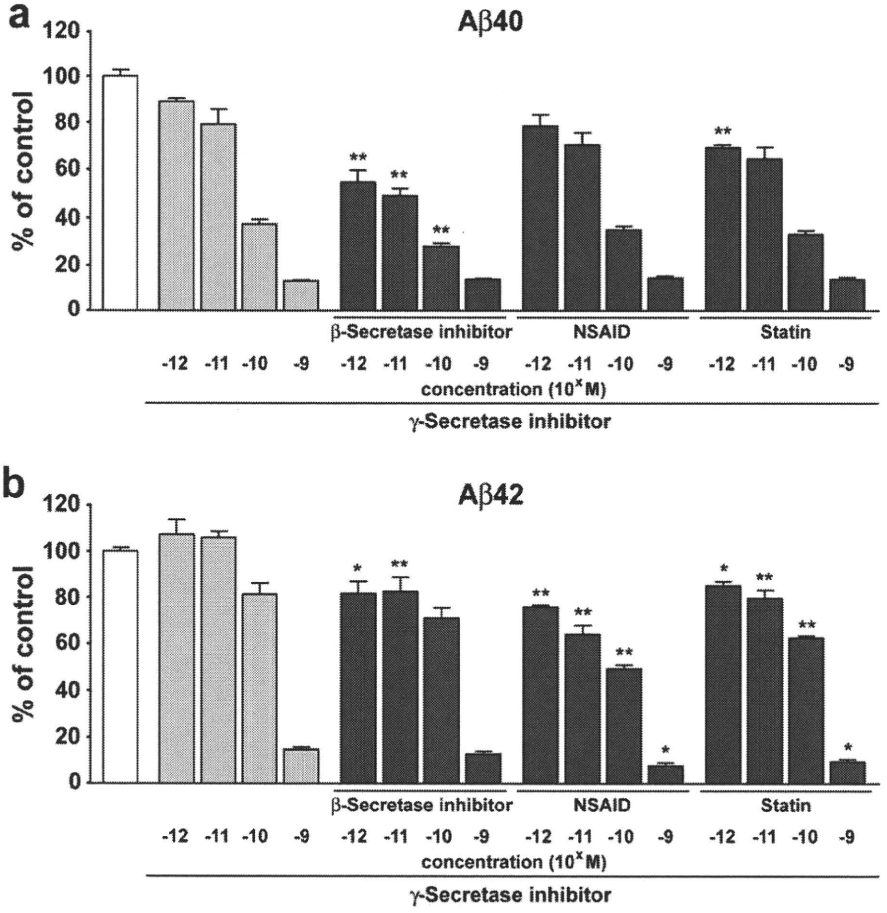

Fig. 3. Effect of the combination of γ-secretase inhibitor with the other drugs on Aβ40 and Aβ42 levels. Amount of Aβ released into the conditioned medium from APP_{NL}-H4 cells treated with each drug in the presence of the γ-secretase inhibitor was measured by sandwich ELISA. Doses of the β-secretase inhibitor, NSAID, and statin were 100 nM, 25 μM, and 1 μM, respectively. Levels of Aβ are expressed as Aβ40 (**a**) and Aβ42 (**b**). Data represent the mean ± SD of three experiments. $*P < 0.05$, $**P < 0.01$, significantly different from group treated with the γ-secretase inhibitor alone at the corresponding concentration.

reduced Aβ42 levels at all doses of the β-secretase inhibitor (Fig. 2b).

Combinatorial Effects of γ-Secretase Inhibitor With One of the Other Drugs on Aβ Production

We examined both Aβ40 and Aβ42 levels in the conditioned media of APP_{NL}-H4 cells treated with the β-secretase inhibitor, NSAID, or statin, in the presence of the γ-secretase inhibitor (Fig. 3). The combinatorial administration of the two secretase inhibitors effectively reduced Aβ40 levels at 10^{-9} to 10^{-6} M of the γ-secretase inhibitor compared with administration of the γ-secretase inhibitor alone (Fig. 3a). At all doses of the γ-secretase inhibitor, however, the NSAID or statin had no additional effects on Aβ40 levels (Fig. 3a). However, these combinations significantly reduced the level of Aβ42 at 10^{-9} to 10^{-6} M of the γ-secretase inhibitor compared with administration of the γ-secretase inhibitor alone (Fig. 3b).

Comparison of the Effects on Aβ Production and the Aβ42/Aβ40 Ratio Between Each Drug and the Four-Drug Cocktail

To assess whether the four-drug cocktail suppressed Aβ production more than each drug alone, we measured the Aβ40 and Aβ42 levels in the conditioned media from APP_{NL}-H4 cells treated with each drug alone or the four-drug cocktail (Fig. 4a–c). The four-drug cocktail acted additively to reduce Aβ40 and Aβ42 levels (Aβ40 level = 23.8% ± 0.6%, Aβ42 level = 28.3% ± 2.8%) with no change in the Aβ ratio (Aβ42/Aβ40 = 118.4% ± 11.7%) compared with the vehicle-treated group (Fig. 4a–c); the observed effects were more prominent than for each drug alone. The β- or γ-secretase inhibitor alone significantly decreased both Aβ40 and Aβ42 levels (β-secretase inhibitor: Aβ40 level = 48.0% ± 5.3%, Aβ42 level = 61.4% ± 7.7%; γ-secretase inhibitor: Aβ40 level = 50.1% ± 9.2%, Aβ42 level = 77.4% ± 9.4%), but they increased the Aβ42/Aβ40 ratio (β-secretase inhibitor: Aβ42/Aβ40 = 127.3% ±

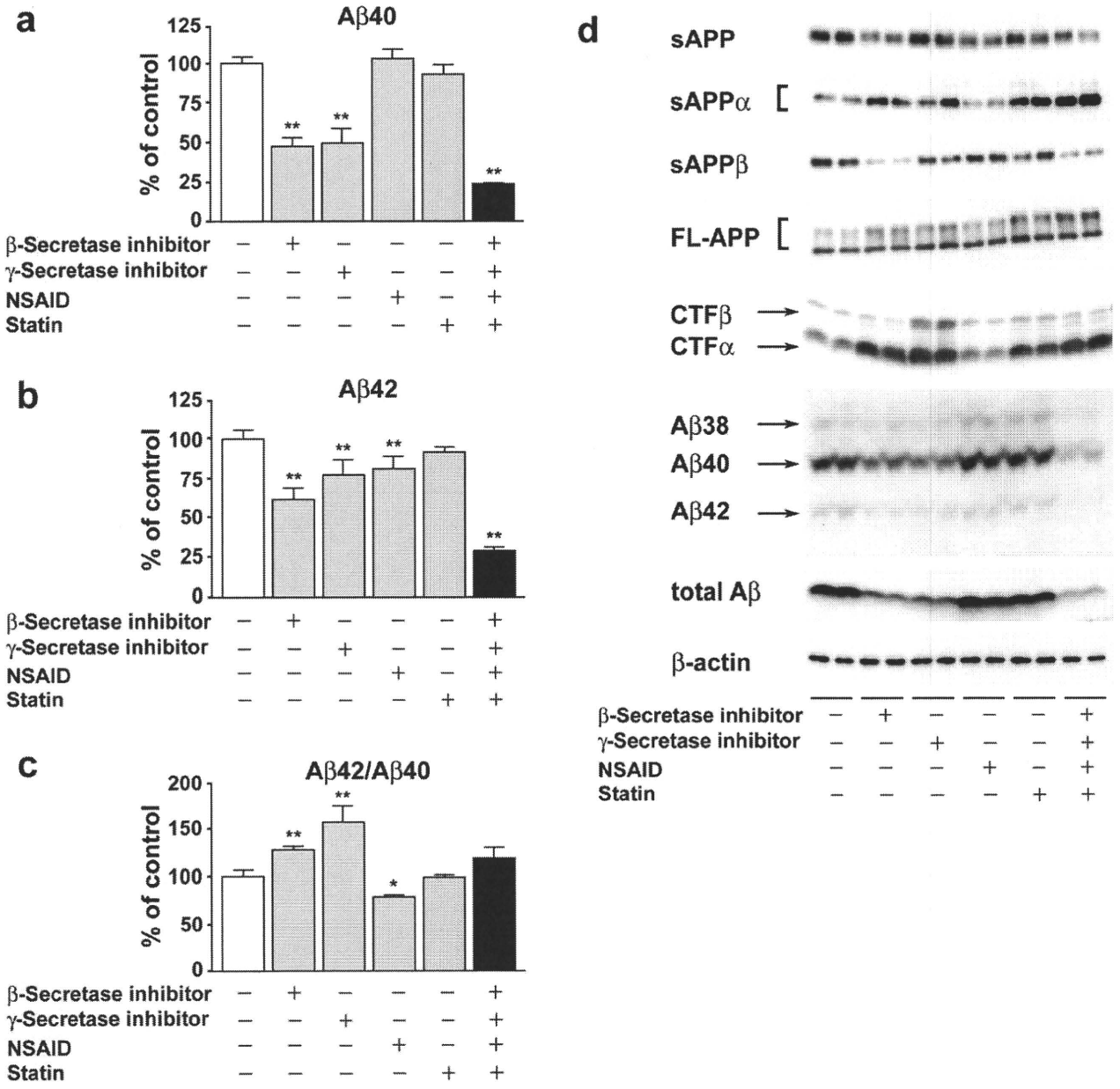

Fig. 4. Comparison of the effects on Aβ production and the Aβ42/Aβ40 ratio for each drug and the four-drug cocktail. Amount of Aβ released into the conditioned medium from APP_{NL}-H4 cells treated with each drug or the four-drug cocktail was measured by sandwich ELISA (a–c). Aβ levels and the Aβ42/Aβ40 ratio are expressed as Aβ40 (**a**), Aβ42 (**b**), and Aβ42/Aβ40 (**c**). Data represent the mean ± SD of four experiments. $*P < 0.05$, $**P < 0.01$, significantly different from the vehicle-treated group (a–c). Results of Western blot analysis for sAPP, sAPPα, sAPPβ, FL-APP, CTFα, CTFβ, Aβ species, total Aβ, and β-actin are shown in **d**. FL, full-length; CTF, C-terminal fragment.

3.8%; γ-secretase inhibitor: Aβ42/Aβ40 = 156.9% ± 18.2%) compared with the vehicle-treated group (Fig. 4a–c). Western blot analysis showed that the four-drug cocktail treatment caused effective decreases in Aβ40, Aβ42, and total Aβ levels and a corresponding increase in sAPPα (Fig. 4d). The four-drug cocktail treatment had no significant effect on cytotoxicity in APP_{NL}-H4 cells (Table I).

Comparison Between the γ-Secretase Inhibitor and Four-Drug Cocktail in Notch Processing and Aβ Levels

γ-Secretase is involved in the intracellular proteolysis of a range of substrates (Beel and Sanders, 2008). Although its inhibitors effectively block Aβ production in vivo and in vitro (Shearman et al., 2000; Beher et al., 2001), they also inhibit the processing of substrate

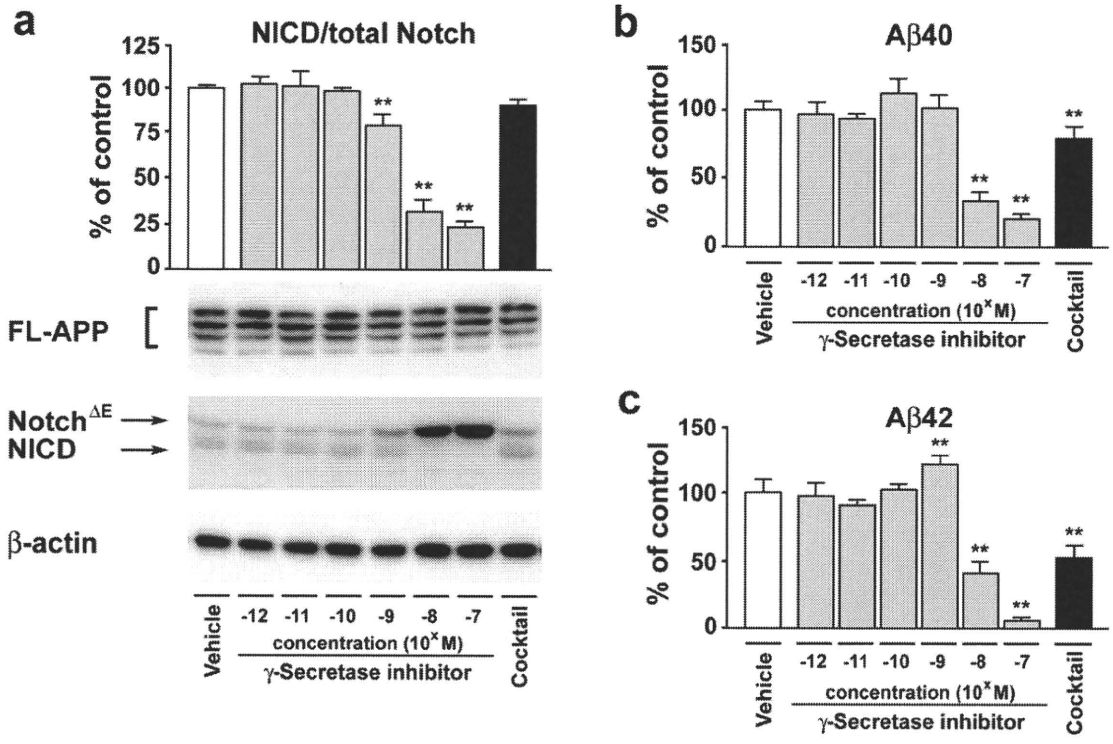

Fig. 5. Comparison between the γ-secretase inhibitor and four-drug cocktail in Notch processing and Aβ40 and Aβ42 levels. Amount of Notch fragments in the cell lysate of mNotch$^{\Delta E}$-N2a cells (**a**) or Aβ released into the conditioned medium from mNotch$^{\Delta E}$-N2a cells (**b,c**) treated with the γ-secretase inhibitor or four-drug cocktail was measured by semiquantitative Western blot analysis or sandwich ELISA, respectively. Data represent the mean ± SD of four experiments (a–c). Sample Western blots are shown for FL-APP, Notch$^{\Delta E}$, NICD, and β-actin (a). Levels of Aβ are expressed as Aβ40 (b) and Aβ42 (c). $^{**}P < 0.01$, significantly different from the vehicle-treated group (a–c). FL, full-length; NICD, Notch intracellular domain.

proteins other than APP as an adverse effect (De Strooper et al., 1999; Geling et al., 2002; Wong et al., 2004). To compare the effects of the four-drug cocktail with that of the γ-secretase inhibitor alone on Notch processing and Aβ production, we investigated the ratio of NICD (Notch intracellular domain) to total Notch and both Aβ40 and Aβ42 levels in the conditioned media from mNotch$^{\Delta E}$-N2a cells by semiquantitative Western blot analysis and sandwich ELISA, respectively (Fig. 5). Notch processing was significantly inhibited by the γ-secretase inhibitor at more than 10^{-9} M. However, the four-drug cocktail treatment had no significant effect on Notch processing (NICD/total Notch = 90.5% ± 3.6%; Fig. 5a) and significantly reduced both Aβ40 and Aβ42 levels (Aβ40 level = 78.8% ± 9.9%, Aβ42 level = 53.3% ± 8.2%) compared with the vehicle-treated group (Fig. 5). In addition, this cocktail treatment was more effective at reducing Aβ42 levels than Aβ40 levels in the mNotch$^{\Delta E}$-N2a cells.

DISCUSSION

Cocktail treatment consists of multiple drugs targeting different sites of action or molecules. It is expected to have an additive or synergistic benefit for therapy and reduce the amount of side effects. This method has been used in an effective manner for AIDS therapy to stop or slow the growth and multiplication of the human immunodeficiency virus and has successfully lowered mortality rates so far. In this study, we have shown that a new pharmacological approach reduces Aβ levels efficiently without adverse effects. This approach is based on the combination of four drugs, β- and γ-secretase inhibitors, NSAID, and statin, targeting distinct processes of Aβ production. The four-drug cocktail reduced Aβ42 levels in the conditioned media of APP_{NL}-H4 and mNotch$^{\Delta E}$-N2a cells. A relative increase in Aβ42 levels causes the accumulation and oligomerization of Aβ42 in the limbic and association cortices in dominantly inherited and sporadic AD; the formation of Aβ42 oligomers is implicated in synaptic dysfunction (Selkoe, 2002). Immunization of APP transgenic mice with synthetic human-type Aβ42 resulted in the removal of Aβ deposits from the brain (Schenk et al., 1999) and could lead to a reversal of cognitive deficits (Morgan et al., 2000). Thus, inhibition of the production and deposition of Aβ42 represents a straightforward strategy for the prevention and therapy of AD.

Both β- and γ-secretase inhibitors are capable of efficiently reducing Aβ levels, even if they are used

solely; therefore, the development of secretase inhibitors is an attractive target for therapeutic intervention in AD (Mattson, 2004; Marks and Berg, 2008; Figs. 2–4). However, these secretase inhibitors preferentially inhibit the production of Aβ40 rather than that of Aβ42, resulting in a significant increase in the Aβ42/Aβ40 ratio (Fig. 4). These results are not attributed to the intrinsic nature of the secretase inhibitors used in the present study. In fact, similar results were obtained with other secretase inhibitors (e.g., the β-secretase inhibitor KMI-429 and the γ-secretase inhibitors DAPT and L-685,458; data not shown). In addition, the increase in Aβ levels by a low-dose treatment with the γ-secretase inhibitor, the "Aβ rise" (Shen and Kelleher, 2007; Burton et al., 2008), was observed in mNotch$^{\Delta E}$-N2a cells (Fig. 5). However, the mechanistic details on why secretase inhibitors show a difference in inhibitory activity between Aβ42 and Aβ40 and why γ-secretase inhibitors cause the Aβ rise remain unclear. Given the genetic knowledge on the *PS* gene (Shen and Kelleher, 2007; Wolfe, 2007) and recent studies indicating that Aβ40 inhibits Aβ42 aggregation in vitro and amyloid deposition in vivo (Kim et al., 2007), the administration of β- or γ-secretase inhibitors alone should be conducted cautiously.

NSAIDs are used primarily to treat inflammation, mild-to-moderate pain, and fever by blocking the activity of cyclooxygenase (COX). Interestingly, some NSAIDs directly alter γ-secretase activity to selectively lower Aβ42 levels accompanied by an increase in Aβ38 levels (Weggen et al., 2001; Eriksen et al., 2003). Beyond that, these NSAIDs have no effect on Notch processing (Weggen et al., 2001); consequently, they represent a promising therapeutic agent for AD (Kukar and Golde, 2008). Sulindac sulfide was efficacious in the decrease of Aβ42 levels as well as an increase in the levels of Aβ38 (Figs. 1, 4b,d). This effect of sulindac sulfide was more powerful than observed for indomethacin in APP$_{NL}$-H4 cells (100 μM: sulindac sulfide decreased Aβ42 levels by 84.2% and the ratio of Aβ42/Aβ40 by 72.0%, whereas indomethacin decreased Aβ42 levels by 36.7% and the ratio of Aβ42/Aβ40 by 12.9%; data not shown). As also observed in previous studies (Weggen et al., 2001; Eriksen et al., 2003), the administration of sulindac sulfide alone lowered the Aβ42/Aβ40 ratio in APP$_{NL}$-H4 cells (78.7% ± 3.2% vs. vehicle-treated group; Fig. 4c). The underlying mechanism for the modulation of γ-secretase activity by NSAIDs is emerging: One paper proposed that NSAIDs have an allosteric effect on PS1, which is the protease-active center molecule of γ-secretase, and alter the interaction of PS1-APP by changing the conformation of PS1 (Lleó et al., 2004). NSAIDs also directly bind to the Aβ region of APP to alter the production of Aβ42 and inhibit the aggregation of Aβ (Kukar et al., 2008). Whether NSAIDs target the enzyme, substrate, or both, sulindac sulfide, which is an Aβ42-lowering NSAID, did not compete with the γ-secretase inhibitor (Fig. 3b). At 10^{-9} to 10^{-7} M of the γ-secretase inhibitor, their coadministration significantly reduced the levels of Aβ42 compared with the administration of the γ-secretase inhibitor alone. These results suggest that coadministration is more effective than administration alone.

Statins are drugs that are widely used to lower cholesterol levels. They inhibit the activity of HMG-CoA reductase, which is the rate-limiting enzyme of the mevalonate pathway of cholesterol synthesis. Because Aβ generation occurs in specialized cholesterol-rich membrane subdomains, the cellular cholesterol level appears to be closely associated with Aβ generation (Kaether and Haass, 2004). Namely, a low level of intracellular cholesterol stimulates the nonamyloidogenic pathway, in which α-secretase is involved (Simons et al., 2001). The reason why simvastatin showed little effect on Aβ40 levels in the presence of the γ-secretase inhibitor in the present study remains unclear (Fig. 3a), whereas coadministration with either the β- or the γ-secretase inhibitor efficiently reduced Aβ42 levels (Figs. 2b, 3b). Moreover, statins have provided a new therapeutic concept for the treatment of neuroinflammatory diseases because of their potency in altering GTPase-mediated signaling relevant to inflammatory processes (Zipp et al., 2007). Because amyloid plaques in AD are accompanied by a localized inflammatory response, statins might also be useful drugs because they interfere with the induction of tumor necrosis factor-α and inducible nitric oxide synthase in astrocytic and microglial cell cultures (Blennow et al., 2006; Zipp et al., 2007; Marks and Berg, 2008).

The efficacy of cocktail treatment should be determined by the additive or synergistic effect of drugs and its ability to alleviate possible adverse side effects that may be caused by individual drugs. Our four-drug cocktail significantly reduced Aβ levels, with no change in Notch processing in APP$_{NL}$-H4 and mNotch$^{\Delta E}$-N2a cells (Figs. 4, 5). The theoretical values estimated by the multiplication of the data of each single drug treatment for the inhibitory efficacies of Aβ production are 23.0% (Aβ40) and 35.4% (Aβ42; Fig. 4a,b). These results were close to the values of four-drug cocktail treatment (Aβ40, 23.8%; Aβ42, 28.3%; Fig. 4a,b). It is suggested that the four drugs used in the present study did not interfere with each other in the suppression of Aβ production. Another important point is that the four-drug cocktail treatment did not affect Notch processing accompanied by significant reduction in Aβ levels (Fig. 5). In contrast, the administration of γ-secretase inhibitor alone exerted its effects on the processing of both APP and Notch (Fig. 5). It follows from these results that this four-drug cocktail did not inhibit the processing of Notch and would have few side effects.

In the present study, we focused on drugs that influence Aβ production. Several drugs have been developed to reduce Aβ levels according to the amyloid hypothesis (Walker et al., 2005; Blennow et al., 2006; Marks and Berg, 2008). For example, α-secretase activators are potential drugs that have two dimensions to their action, because α-secretase cleaves within the Aβ region of APP, leading to a reduction in Aβ levels and

the generation of sAPPα that has neuroprotective effects. For the Aβ-degradation system, Saito et al. (2005) reported that the neuropeptide somatostatin regulates Aβ catabolism by modulating the activity and localization of neprilysin, which is a major enzyme responsible for the degradation of Aβ (Iwata et al., 2001). Therefore, somatostatin receptors might be new pharmacological target molecules for the prevention and treatment of AD (Iwata et al., 2005; Saido and Iwata, 2006). For the Aβ-clearance system (Aβ efflux system from the brain parenchyma to peripheral blood), it is becoming clear that a particularly promising approach for the removal of Aβ is to use the power and specificity of the immune system to eliminate excess Aβ in the brain (Town, 2009). Although immunization with Aβ resulted in clearance of amyloid plaques in the brains of AD patients, the clearance did not present significant improvement of the patients' cognitive functions. It is thought that one of major causes that have driven Aβ immunotherapy into failure may be targeting to eliminate amyloid plaques per se. Increasing evidence has indicated that particular forms of soluble Aβ, such as oligomeric froms, but not insoluble Aβ, may be one of major causes leading to neuronal dysfunction and further cognitive impairment (Haass and Selkoe, 2007). Thus, it is suggested that it may be necessary to inhibit newly produced Aβ, which forms soluble oligomers. In addition, compounds capable of disaggregating Aβ or inhibiting Aβ aggregation (formation of low-molecular-weight oligomers and fibrils) are pharmacological strategies that could be used in the treatment of AD. Recently, it was reported that the reduction of pyroglutamate-modified Aβ by inhibition of glutaminyl cyclase offered an attenuation of AD-like pathology in AD model mice and a new *Drosophila* model (Schilling et al., 2008). Large numbers of drugs have been developed in recent years, and numerous options for combinatorial therapies are available to reduce Aβ levels without leading to adverse effects, such as the impairment of Notch processing, as shown here. Some clinical trials of an Aβ-targeting compound have failed (for example, *R*-flurbiprofen; Green et al., 2009). However, almost all of the compounds have been administered alone. Our data suggest that administration of a combination of drugs consisting of Aβ-lowering drugs at low doses such as our four-drug cocktail might be an effective approach by which to prevent, delay, slow, and treat AD. This cocktail strategy may be extended to targeting the other downstream pathological processes of AD, such as tauopathy, oxidative stress, inflammation, neuronal loss, and neuronal cell death, to achieve maximal effects (Saido and Iwata, 2006). We suggest that a transition might be coming from the time when a single drug is developed and evaluated to the time when multiple drugs are designed.

ACKNOWLEDGMENTS

We thank Dr. Raphael Kopan (Washington University) for providing the plasmid of mNotch$^{\Delta E}$ and Mr. Sosuke Yagishita (The University of Tokyo) for his valuable technical advice.

REFERENCES

Asai M, Hattori C, Iwata N, Saido TC, Sasagawa N, Szabó B, Hashimoto Y, Maruyama K, Tanuma S, Kiso Y, Ishiura S. 2006. The novel β-secretase inhibitor KMI-429 reduces amyloid β peptide production in amyloid precursor protein transgenic and wild-type mice. J Neurochem 96:533–540.

Asai M, Iwata N, Yoshikawa A, Aizaki Y, Ishiura S, Saido TC, Maruyama K. 2007. Berberine alters the processing of Alzheimer's amyloid precursor protein to decrease Aβ secretion. Biochem Biophys Res Commun 352:498–502.

Beel AJ, Sanders CR. 2008. Substrate specificity of γ-secretase and other intramembrane proteases. Cell Mol Life Sci 65:1311–1334.

Beher D, Wrigley JD, Nadin A, Evin G, Masters CL, Harrison T, Castro JL, Shearman MS. 2001. Pharmacological knock-down of the presenilin 1 heterodimer by a novel γ-secretase inhibitor: implications for presenilin biology. J Biol Chem 276:45394–45402.

Blennow K, de Leon MJ, Zetterberg H. 2006. Alzheimer's disease. Lancet 368:387–403.

Burton CR, Meredith JE, Barten DM, Goldstein ME, Krause CM, Kieras CJ, Sisk L, Iben LG, Polson C, Thompson MW, Lin XA, Corsa J, Fiedler T, Pierdomenico M, Cao Y, Roach AH, Cantone JL, Ford MJ, Drexler DM, Olson RE, Yang MG, Bergstrom CP, McElhone KE, Bronson JJ, Macor JE, Blat Y, Grafstrom RH, Stern AM, Seiffert DA, Zaczek R, Albright CF, Toyn JH. 2008. The amyloid-β rise and γ-secretase inhibitor potency depend on the level of substrate expression. J Biol Chem 283:22992–23003.

De Strooper B, Annaert W, Cupers P, Saftig P, Craessaerts K, Mumm JS, Schroeter EH, Schrijvers V, Wolfe MS, Ray WJ, Goate A, Kopan R. 1999. A presenilin-1-dependent γ-secretase-like protease mediates release of Notch intracellular domain. Nature 398:518–522.

Dominguez D, Tournoy J, Hartmann D, Huth T, Cryns K, Deforce S, Serneels L, Camacho IE, Marjaux E, Craessaerts K, Roebroek AJ, Schwake M, D'Hooge R, Bach P, Kalinke U, Moechars D, Alzheimer C, Reiss K, Saftig P, De Strooper B. 2005. Phenotypic and biochemical analyses of BACE1- and BACE2-deficient mice. J Biol Chem 280:30797–30806.

Eriksen JL, Sagi SA, Smith TE, Weggen S, Das P, McLendon DC, Ozols VV, Jessing KW, Zavitz KH, Koo EH, Golde TE. 2003. NSAIDs and enantiomers of flurbiprofen target γ-secretase and lower Aβ42 in vivo. J Clin Invest 112:440–449.

Fassbender K, Simons M, Bergmann C, Stroick M, Lutjohann D, Keller P, Runz H, Kuhl S, Bertsch T, von Bergmann K, Hennerici M, Beyreuther K, Hartmann T. 2001. Simvastatin strongly reduces levels of Alzheimer's disease β-amyloid peptides Aβ42 and Aβ40 in vitro and in vivo. Proc Natl Acad Sci U S A 98:5856–5861.

Geling A, Steiner H, Willem M, Bally-Cuif L, Haass C. 2002. A γ-secretase inhibitor blocks Notch signaling in vivo and causes a severe neurogenic phenotype in zebrafish. EMBO Rep 3:688–694.

Green RC, Schneider LS, Amato DA, Beelen AP, Wilcock G, Swabb EA, Zavitz KH,Tarenflurbil Phase 3 Study Group. 2009. Effect of tarenflurbil on cognitive decline and activities of daily living in patients with mild Alzheimer disease: a randomized controlled trial. JAMA 302:2557–25564.

Haass C, Selkoe DJ. 2007. Soluble protein oligomers in neurodegeneration: lessons from the Alzheimer's amyloid β-peptide. Nat Rev Mol Cell Biol 8:101–112.

Imamura Y, Watanabe N, Umezawa N, Iwatsubo T, Kato N, Tomita T, Higuchi T. 2009. Inhibition of γ-secretase activity by helical β-peptide foldamers. J Am Chem Soc 131:7353–7359.

Iwata N, Tsubuki S, Takaki Y, Shirotani K, Lu B, Gerard NP, Gerard C, Hama E, Lee HJ, Saido TC. 2001. Metabolic regulation of brain Aβ by neprilysin. Science 292:1550–1552.

Iwata N, Higuchi M, Saido TC. 2005. Metabolism of amyloid-β peptide and Alzheimer's disease. Pharmacol Ther 108:129–148.

Kaether C, Haass C. 2004. A lipid boundary separates APP and secretases and limits amyloid β-peptide generation. J Cell Biol 167:809–812.

Kim J, Onstead L, Randle S, Price R, Smithson L, Zwizinski C, Dickson DW, Golde T, McGowan E. 2007. Aβ40 inhibits amyloid deposition in vivo. J Neurosci 27:627–633.

Kopan R, Schroeter EH, Weintraub H, Nye JS. 1996. Signal transduction by activated mNotch: importance of proteolytic processing and its regulation by the extracellular domain. Proc Natl Acad Sci U S A 93:1683–1688.

Kukar T, Golde TE. 2008. Possible mechanisms of action of NSAIDs and related compounds that modulate γ-secretase cleavage. Curr Top Med Chem 8:47–53.

Kukar TL, Ladd TB, Bann MA, Fraering PC, Narlawar R, Maharvi GM, Healy B, Chapman R, Welzel AT, Price RW, Moore B, Rangachari V, Cusack B, Eriksen J, Jansen-West K, Verbeeck C, Yager D, Eckman C, Ye W, Sagi S, Cottrell BA, Torpey J, Rosenberry TL, Fauq A, Wolfe MS, Schmidt B, Walsh DM, Koo EH, Golde TE. 2008. Substrate-targeting γ-secretase modulators. Nature 453:925–929.

Lleó A, Berezovska O, Herl L, Raju S, Deng A, Bacskai BJ, Frosch MP, Irizarry M, Hyman BT. 2004. Nonsteroidal anti-inflammatory drugs lower $A\beta_{42}$ and change presenilin 1 conformation. Nat Med 10:1065–1066.

Marks N, Berg MJ. 2008. Neurosecretases provide strategies to treat sporadic and familial Alzheimer disorders. Neurochem Int 52:184–215.

Mattson MP. 2004. Pathways towards and away from Alzheimer's disease. Nature 430:631–639.

Morgan D, Diamond DM, Gottschall PE, Ugen KE, Dickey C, Hardy J, Duff K, Jantzen P, DiCarlo G, Wilcock D, Connor K, Hatcher J, Hope C, Gordon M, Arendash GW. 2000. Aβ peptide vaccination prevents memory loss in an animal model of Alzheimer's disease. Nature 408:982–985.

Saido TC, Iwata N. 2006. Metabolism of amyloid β peptide and pathogenesis of Alzheimer's disease. Towards presymptomatic diagnosis, prevention and therapy. Neurosci Res 54:235–253.

Saito T, Iwata N, Tsubuki S, Takaki Y, Takano J, Huang SM, Suemoto T, Higuchi M, Saido TC. 2005. Somatostatin regulates brain amyloid β peptide $A\beta_{42}$ through modulation of proteolytic degradation. Nat Med 11:434–439.

Schenk D, Barbour R, Dunn W, Gordon G, Grajeda H, Guido T, Hu K, Huang J, Johnson-Wood K, Khan K, Kholodenko D, Lee M, Liao Z, Lieberburg I, Motter R, Mutter L, Soriano F, Shopp G, Vasquez N, Vandevert C, Walker S, Wogulis M, Yednock T, Games D, Seubert P. 1999. Immunization with amyloid-β attenuates Alzheimer-disease-like pathology in the PDAPP mouse. Nature 400:173–177.

Schilling S, Zeitschel U, Hoffmann T, Heiser U, Francke M, Kehlen A, Holzer M, Hutter-Paier B, Prokesch M, Windisch M, Jagla W, Schlenzig D, Lindner C, Rudolph T, Reuter G, Cynis H, Montag D, Demuth HU, Rossner S. 2008. Glutaminyl cyclase inhibition attenuates pyroglutamate Aβ and Alzheimer's disease-like pathology. Nat Med 14:1106–1111.

Seiffert D, Bradley JD, Rominger CM, Rominger DH, Yang F, Meredith JE Jr, Wang Q, Roach AH, Thompson LA, Spitz SM, Higaki JN, Prakash SR, Combs AP, Copeland RA, Arneric SP, Hartig PR, Robertson DW, Cordell B, Stern AM, Olson RE, Zaczek R. 2000. Presenilin-1 and -2 are molecular targets for γ-secretase inhibitors. J Biol Chem 275:34086–34091.

Selkoe DJ. 2002. Alzheimer's disease is a synaptic failure. Science 298:789–791.

Shearman MS, Beher D, Clarke EE, Lewis HD, Harrison T, Hunt P, Nadin A, Smith AL, Stevenson G, Castro JL. 2000. L-685,458, an aspartyl protease transition state mimic, is a potent inhibitor of amyloid β-protein precursor γ-secretase activity. Biochemistry 39:8698–8704.

Shen J, Kelleher RJ 3rd. 2007. The presenilin hypothesis of Alzheimer's disease: evidence for a loss-of-function pathogenic mechanism. Proc Natl Acad Sci U S A 104:403–409.

Simons M, Keller P, Dichgans J, Schulz JB. 2001. Cholesterol and Alzheimer's disease: is there a link? Neurology 57:1089–1093.

Stachel SJ, Coburn CA, Steele TG, Jones KG, Loutzenhiser EF, Gregro AR, Rajapakse HA, Lai MT, Crouthamel MC, Xu M, Tugusheva K, Lineberger JE, Pietrak BL, Espeseth AS, Shi XP, Chen-Dodson E, Holloway MK, Munshi S, Simon AJ, Kuo L, Vacca JP. 2004. Structure-based design of potent and selective cell-permeable inhibitors of human β-secretase (BACE-1). J Med Chem 47:6447–6450.

Town T. 2009. Alternative Aβ immunotherapy approaches for Alzheimer's disease. CNS Neurol Disord Drug Targets 8:114–127.

Walker LC, Ibegbu CC, Todd CW, Robinson HL, Jucker M, LeVine H 3rd, Gandy S. 2005. Emerging prospects for the disease-modifying treatment of Alzheimer's disease. Biochem Pharmacol 69:1001–1008.

Weggen S, Eriksen JL, Das P, Sagi SA, Wang R, Pietrzik CU, Findlay KA, Smith TE, Murphy MP, Bulter T, Kang DE, Marquez-Sterling N, Golde TE, Koo EH. 2001. A subset of NSAIDs lower amyloidogenic Aβ42 independently of cyclooxygenase activity. Nature 414:212–216.

Weggen S, Rogers M, Eriksen J. 2007. NSAIDs: small molecules for prevention of Alzheimer's disease or precursors for future drug development. Trends Pharmacol Sci 28:536–543.

Willem M, Garratt AN, Novak B, Citron M, Kaufmann S, Rittger A, De Strooper B, Saftig P, Birchmeier C, Haass C. 2006. Control of peripheral nerve myelination by the β-secretase BACE1. Science 314:664–666.

Wolfe MS. 2007. When loss is gain: reduced presenilin proteolytic function leads to increased Aβ42/Aβ40. Talking point on the role of presenilin mutations in Alzheimer disease. EMBO Rep 8:136–140.

Wong GT, Manfra D, Poulet FM, Zhang Q, Josien H, Bara T, Engstrom L, Pinzon-Ortiz M, Fine JS, Lee HJ, Zhang L, Higgins GA, Parker EM. 2004. Chronic treatment with the γ-secretase inhibitor LY-411,575 inhibits β-amyloid peptide production and alters lymphopoiesis and intestinal cell differentiation. J Biol Chem 279:12876–12882.

Zipp F, Waiczies S, Aktas O, Neuhaus O, Hemmer B, Schraven B, Nitsch R, Hartung HP. 2007. Impact of HMG-CoA reductase inhibition on brain pathology. Trends Pharmacol Sci 28:342–349.

特集1

プロテアーゼ依存性細胞シグナリングと生理・病態

膜結合型メタロプロテアーゼ（MMP, ADAM）ファミリー

二井勇人（ふたいゆうじん），石浦章一（いしうらしょういち）｜東京大学大学院総合文化研究科広域科学専攻生命環境科学系（〒153-8902 東京都目黒区駒場3-8-1）
E-mail：futai@bio.c.u-tokyo.ac.jp

SUMMARY

膜結合型メタロプロテアーゼには，MT-MMP（Membrane Type- Matrix Metalloprotease）とADAM（A Disintegrin And Metalloprotease）が知られている．このうちのADAMは，プロテアーゼ活性中心を担うメタロプロテアーゼドメイン以外に，複数のドメイン構造を持ち，細胞表面で重要な機能をはたす多機能調節因子として注目されている．膜型成長因子，細胞接着因子など膜タンパク質の細胞外領域を切断する反応は，細胞外ドメイン“シェディング”（ectodomain shedding）と呼ばれ，限定分解された基質は細胞内シグナリングにおいて新しい機能を獲得する．本章では，特にADAMファミリーに焦点を当て，シグナリングにおける機能・病態における役割を紹介する．

KEY WORDS

ADAM
シェディング
細胞内シグナリング
RIP
アルツハイマー病

I. ADAMファミリープロテアーゼのドメイン構造

ADAM（A Disintegrin And Metalloprotease）は，名前からも分かるように，Disintegrinドメインとメタロプロテアーゼドメインをひとつずつ有している．加えて，アミノ末端のシグナルペプチドとProドメイン，そしてCysteine-richドメインとEGF様ドメインを持つ．DisintegrinとCysteine-richドメインは，インテグリン等の蛋白質との相互作用において機能する（**図1**）．プロテアーゼドメインによるタンパク質限定分解だけでなく，細胞外でのタンパク質相互作用による細胞間，細胞マトリックス間の接着に重要な役割を果たしている．MT-MMPと比較しても，これらの多ドメイン構造による多機能性は，ADAMファミリーにおいて顕著な特徴である．これまでにADAM1～ADAM40まで，40個のADAMが見出されている[1]（http://www.people.virginia.edu/~jw7g/Table_of_the_ADAMs.html参照）．このうち約6割が，プロテアーゼ活性を持つと考えられているが，残りはプロテアーゼ活性中心を持たず，DisintegrinとCysteine-richドメインを介した細胞接着機能をもつと考えられる．プロテアーゼ不活性化型ADAMの生理機能は，遺伝子破壊マウスを用いた解析等からも解明されている（**表1-2**，ADAM2, 3, 11, 22, 23はプロテアーゼ不活性）．ADAMは種々の生

1344-0128/10/¥100/頁/JCOPY

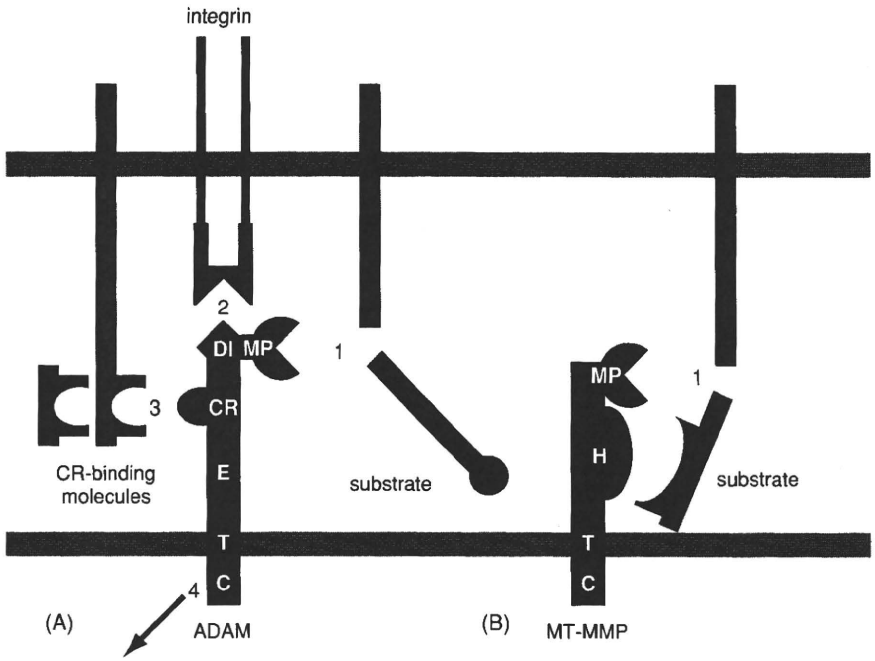

図1　ADAMとMT-MMPのドメイン構造

A：ADAMの各ドメインの機能に付いて，(1) メタロプロテアーゼ（MP）ドメインの触媒部位による基質の切断 (2) disintegrinドメイン（DI）とインテグリンヘテロ二量体との結合 (3) Cytein-richドメイン（CR）を介した他の蛋白質との相互作用 (4) いくつかのADAMにおいて見られる細胞質ドメイン（C）を経由した細胞内情報伝達を示している．以上の機能ドメインと膜貫通領域（T）に加えて，EGF様ドメイン（E）を有する分子も見つかっている．B：MT-MMPの各ドメインでは，ADAMと同様に（1）MPドメインを介した基質の切断の他に，ヘモペキシンドメイン（H）を介した他の蛋白質（CD44等の基質）との相互作用が知られている．（文献1)より改変）

物種から同定が試みられており，ヒトから*Drosophila*，線虫まで全ての多細胞生物で存在が見出されている．また，*Aspergillus*等の菌類や，単細胞生物では分裂酵母*Schizoscchаromyces pombe*にもADAMと相同性を有するADAM様プロテアーゼが存在する．（出芽酵母*Saccharomyces cerevisiae*には，ホモログは存在しない．）分裂酵母のMde10は，胞子形成に必須である事が知られている[4]．

II. ADAMの活性制御機構

ADAMの活性制御機構についてであるが，ADAMは，MT-MMP等と同様，プロテアーゼ不活性な前駆体として合成される．輸送過程で，アミノ末端のProドメインがエンドペプチダーゼ（Furin等）により切断されて，はじめて活性を持つ．ADAM8とADAM28では，自己消化によってもProドメインが切除される．また，ADAMによる蛋白分解には，構成的なシェディングに加え，G蛋白質共役型受容体リガンド，PKC活性化剤（PMA：phorbor myristate acetate），カルシウムイオノフォアなどで誘導される調節的シェディングが知られている[5]．しかし，ADAMの細胞内ドメインが修飾を受けて活性化を受ける機構にはまだ良く分かっていない点が多い．

III. シェディングの生理的意義

近年，ADAMによりシェディングを受ける基質は多数見つかってきている（**表1-1**）．以下では，その生理的意義について，例を挙げて解説する．

シェディングがもたらす機能は，基質により大きく異なり，以下の4つの機能が考えられる．(1) シェディングによるサイトカインや成長因子（TNFα，EGFRリガンドなど）の切断・放出は，分泌細胞自身や近接

する細胞への情報伝達を引き起こす．(2) 反対に，受容体の切断は，シグナリングの不活性化をもたらし，放出された可溶性受容体はデコイ受容体（リガンドの効果を中和する）として機能する事も考えられる．ADAMには，リガンドと受容体双方を基質とする例が多く知られている（表1-1）．(3) シェディングに続いて膜内切断（RIP : regulated intramembrane proteolysis）が起こり，切断された細胞内領域による細胞内情報伝達が開始する．(4) 細胞間もしくは細胞とマトリックス間の接着に機能する接着因子が切断されると，結合が解離して細胞機能へと影響を与える．*Xenopus* ADAM13は，発生過程で神経細胞の移動に必要であることが明確に示されている[6]．

1. シェディングによる情報伝達：EGFシグナリング系

G蛋白質共役型受容体（GPCR）の活性化に伴うEGFシグナリング系の活性化（transactivation）には，ADAMの活性が必要である事が知られている．EGF受容体リガンドには，ヘパリン結合型EGF（HB-EGF），proTGFα，amphiregulin等が知られているが，GPCRの活性化に伴い，これらの膜結合型成長因子がシェディングを受けて細胞外に放出され，近傍の細胞もしくは自身の細胞表面にあるEGFRを活性化するというのがこの情報伝達系の概要である（**図2A**）．HB-EGF，proTGFα，amphiregulinのシェディングには複数のADAM（9, 10, 12, 15, 17, 19）が関与する事が，培養細胞等を用いた解析から明らかになっている[7]．しかし．遺伝子欠損マウスを用いた解析から（表1-2），ADAM17欠損マウス（生後約17.5日で死亡する）に眼瞼形成不全，毛髪・皮膚形成不全，複数の臓器での上皮組織成熟不全がみられ，これらの全てが，EGFR欠損マウスおよびEGFリガンド欠損マウスの表現型と似通ったものである事から，生体内ではADAM17が主要なHB-EGFの切断酵素であろうと考えられるようになった[2]．GPCRによる活性化がADAMの活性化を引き起こす機

表1-1　ADAMの基質

ADAM	Substrates
8	CD23, CD30-ligand (CD153), CHL1, L-selectin, ADAM8 (prodomain cleavage)
9	pro-EGF, proHB-EGF, FGF-receptor2, Kit ligand, p75 neutrophin receptor (NTR), Insulin B chain, Delta-1, IGFBP-5, APP, oxytocinase, collagen XVII, fibronectin, laminin, ADAM10
10	proTNFα, proEGF, proHB-EGF, probetacellulin, proTGFα, pro-betacellulin, TRANCE/RANKL, IL-6R, Notch, Delta1, fractalkine (CX3CL1), CXCL16, LAG-3, desmoglein-2, klotho, ephrin-A2, c-Met, Fas-ligand, erbB2/HER2, Thyrotopin Receptor (TSHR), CD23, CD30, CD44, L1 adhesion molecule, N-cadherin, E-cadherin, Proto-cadhelin γ C3 and B4, VE-cadherin, APP, Prion Protein Cellular (PrPc), collagen XVII
12	proHB-EGF,IGFBP-3, IGFBP-5, oxytocinase, fibronectin, collagen IV, gelatin, Delta-1, Scarboxymethylated transferrin
13	fibronectin, ADAM13 (cysteine-rich domain)
15	pro-HB-EGF, proamphiregulin, proTGFα, CD23, E-cadherin, collagen IV
17	proTNFα, proHB-EGF, proTGFα, proamphiregulin, proepiregulin, proneuregulin α2c, epigen, CD30, CD40, p55 TNFR, p75TNFR, p75 NTR, TrkA, TRANCE/RANKL, c-Kit, Kit ligand-1 and 2, erbB4/HER4, GHR, IL-1R, IL-6R, IL-15Rα, M-CSFR, Notch, Delta-1CX3CL1, CX3CL1, LAG-3, CSF-1, CD30, CD40, CD44, L-selectin, nectin-4MUC1, VCAM-1, L1-CAM, N-CAM, PTP-LAR, Pref-1, ACE2/SARS-CoV Receptor, Semaphorin 4D, neuronal pentraxin receptor (NPR), ALCAM, Desmoglein, Klotho, Vps10, GP1b-α, APP, Ebola Glycoprotein, PrPc, Vibrio cholera cytolysin, collage XVII
19	proTNFα (in ADAM17 deficient cells), neuregulin, TRANCE/RANKL, ADAM19 (cysteinerich domain)
28	CD23, IGFBP-3, ADAM28 (prodomain)
33	kit-ligand 1, CD23, APP

表1-2　ADAMノックアウトマウス

ADAM	Phenotype
1a	Male infertility, defect in sperm migration
2	Male infertility, defect in sperm migration and adhesion, defect in migration of neuroblasts to olfactory bulb
3	Male infertility, defect in sperm migration and adhesion
8	Viable, fertile, no pathology (reduced CHL-1 shedding in brain)
9	Viable, fertile, no pathology
10	Early lethality (E9.5), defective CNS and heart development, somite formation and vasculogenesis. Phenocopied to Notch deficiency (severe than presenilin 1 and 2 double knockouts).
11	Viable, fertile, impaired hippocampal-dependent spatial learning and altered nociception responces.
12	Viable, fertile, 30% embryonic lethality, brown adipose abnormalities, no muscle defect.
15	Vialble, fertile, tumor neovascularization reduced, age onset osteoarthritis.
17	Perinatal lethality, probably due to heart defects; pulmonary hypoplasia; problems with epithelial tissue maturation. Phenocopies defects seen in EGFR, TGFα, HB-EGF and amphiregulin knockout mice.
19	80% postnatal lethality, multiple cardiovascular defects.
22	Postnatal lethality, multiple cardiovascular defects.
23	Postnatal lethality, multiple cardiovascular defects.
33	Viable, fertile, no pathology.

（文献2), 3)より引用，改変）

構についても，Ras-ERK経路，PKC，p38MAPキナーゼ等によるシェディングの誘導が知られ，ADAM17の細胞質ドメインのリン酸化についての解析が進んでいる．**図2A**にはGPCRの活性化後，Src，PI3-kinaseとPI-dependent kinase-1（PDK1）が順に活性化され，ADAM17をリン酸化する事を示したZhangらによる結果を示した[8]．

2. シェディングからRIPへの段階的切断：Notchシグナリング系

ADAMによるシェディングを受ける膜蛋白質のうち多くは，シェディングに引き続きγ-セクレターゼによって膜内切断（RIP）を受ける．γ-セクレターゼは，presenilin1とpresenilin2が活性中心となるアスパラギン酸プロテアーゼである．代表的な基質であるNotchは，細胞膜への輸送過程でpro-protein convertase（Furin）により切断された後，細胞表面でヘテロ2量体を形成する．そして，Notchリガンド（DeltaやJagged等）の結合により活性化され，ADAMによるシェディング，γ-セクレターゼによる膜内切断を段階的に受ける．切断された細胞内領域は，核に移行して下流の遺伝子の転写活性化に機能する[2]（**図2B**）．Notchのシェディングに関与するADAMについては，複数のADAMがNotchを切断する事が分かっているが（表1-1），遺伝子欠損マウスを用いた解析から，ADAM10が主要なNotch切断酵素であろうと考えられている．ADAM10欠損マウスは，胚性致死（E9.5）となり，神経系，循環器系，体節の形成不全を示すが，これはNotch/Delta情報伝達を欠損するマウスで見られる表現型ととても良く似ている（表1-2）．*Drosophilla*のKuzbanianや線虫のSup-17等，遺伝的手法でNotchとの関連が同定された遺伝子も，ADAM-10のホモログである事から，この情報伝達系が種を超えて保存されている事が分かる．シェディングに続いてRIPを受ける蛋白質としては，Notchの他にNotchのリガンドのDeltaがあげられる．Deltaのシェディングは，リガンドの除去によりNotchシグナリングの空間的制御を

する一方，RIPを引き起こし，細胞内断片は核内に移行する事も知られている．他にもCD44，L1，erbB4，amyloid precursor protein（APP）は，細胞内領域に転写活性化能を持つ蛋白質でNotchと同様の転写誘導が示唆されている．N-カドヘリンでは，細胞内領域と結合するβ-カテニンがシェディングに伴い核へ移行し，遺伝子の転写を制御する．

IV. 病態における役割

これまでに，ADAMは，がん，炎症（リウマチなど），喘息，アルツハイマー病など，種々の病態における機能が示唆されている．

1. がん細胞の増殖，転移

腫瘍組織またはがん細胞では，ADAM 8, 9, 10, 12, 15, 17, 19, 28の発現の上昇が報告されている[9]．また，ADAM12は，乳癌の原因遺伝子としても同定され，変異により細胞表面への輸送異常がおこり，基質の切断が阻害される事が確認されている[10]．今後はどの基質の切断が腫瘍の増殖と転移において重要であるかを明確にしていく必要があると考えられる．メタロプロテアーゼ阻害によるがんの治療は，これまでにその特異性の低さが問題になってきたが，ADAM特異的メタロプロテアーゼ阻害剤による治療が期待される．

2. アルツハイマー病でのアミロイド（Aβ）産生への関与

アミロイド前駆体蛋白質（APP）は，細胞内での代

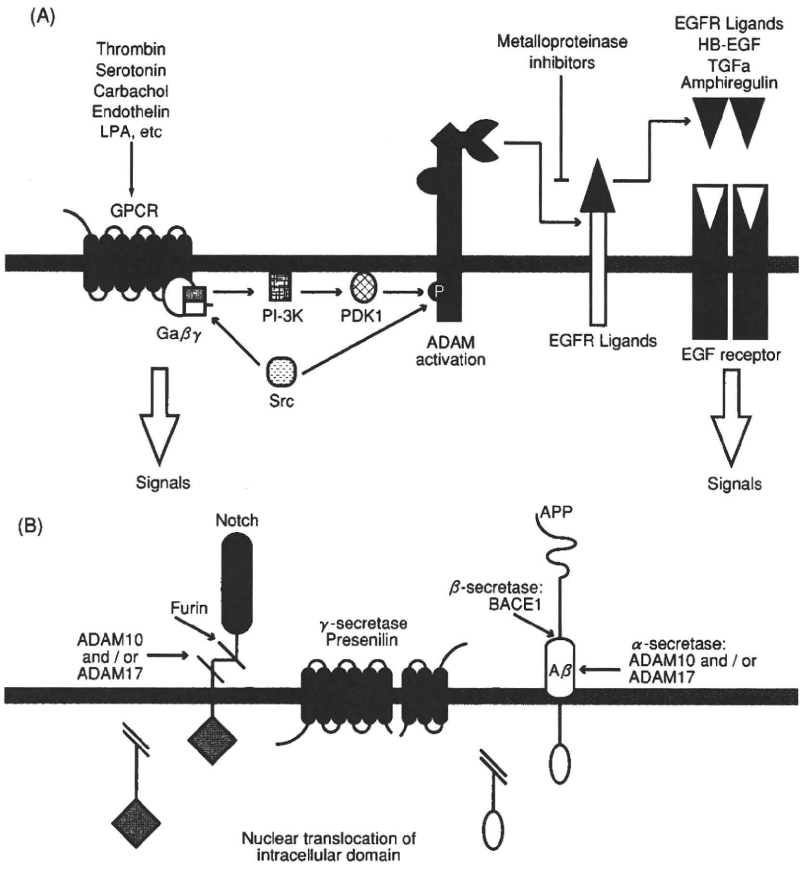

図2

（A）EGFRリガンドのシェディングによる活性化とGPCR経路のクロストーク．Zhangらの解析(8)により示唆されたモデルである．（B）Notchとアミロイド前駆体タンパク質（APP）の膜内切断（RIP: Regurated intramembrane proteolysis）．詳細は本文を参照．（文献2)より改変）